Relative sea-level rise and the influence of vertical land motion at Tropical Pacific Islands

Adrian Martínez-Asensio, Guy Woppelmann, Valérie Ballu, Melanie Becker, Laurent Testut, Alexandre K. Magnan, Virginie Duvat

Relative sea-level rise and the influence of vertical land motion at Tropical Pacific Islands

A. Martinez-Asensio*[1], G. Wöppelmann[1], V. Ballu[1], M. Becker, [1] L. Testut[1,2], A.K. Magnan[3,1], V.K.E. Duvat[1]

[1] LIENSs, University of La Rochelle / CNRS, la Rochelle, France

[2] LEGOS, University of Toulouse, CNES, CNRS, IRD, UPS, Toulouse, France

[3] Institute for Sustainable Development and International Relations (IDDRI), Paris, France

*Corresponding author: admartinezasensio@gmail.es

Abstract

This study investigates the relative sea-level changes and the influence of vertical land movements at South Western Tropical Pacific Islands. The dataset consists of tide gauge records, remote satellite altimetry observations and GPS records. After evaluating the uncertainties and the nature of vertical land movements, we focus on the present and future relative sea-level changes. The main source of uncertainty comes from the types of vertical land motion estimates. Results revealed that the relative sea level has increased more than the global mean sea level (from 0.8 to 4.2 mm yr^{-1} higher) overall in the region during the last 4-6 decades, especially at the islands located over the most tectonically active areas where future changes cannot be reliably projected. For most of the islands located outside tectonically active areas, relative sea-level projected changes by the end of the 21st century are of similar magnitude to the projected global mean sea-level (0.6 ± 0.2 m in the RCP 8.5 scenario), with the exception of Tahiti where major changes are projected (0.8 ± 0.2 m).

1. Introduction

Small Pacific island nations and in particular atoll nations have received much attention during the recent decades given their high exposure to sea-level rise (SLR) in the context of climate change (Nurse et al., 2014; Connell et al., 2015; Duvat et al., 2017). Despite the absence of scientific evidence of direct correlation between atoll island shoreline retreat and sea-level rise (McLean and Kench, 2015; Duvat, 2018), SLR superimposed with zonal extreme events (i.e. tropical cyclones) and distant-source wave intensification is expected to increase coastal erosion, marine flooding and soil and groundwater lens salinization. This will also be exacerbated by a decrease in the resilience of reef ecosystems (Keener et al., 2012;

Saunders et al., 2016; Shope et al., 2016 and references herein). In this region, sea-level changes are thus a key concern about the long-term adaptation to climate change issue.

The rate of global sea-level rise due to thermal expansion and melting ice sheets and glaciers has been significantly higher during the altimetry period (1993-2012) [3.2 ± 0.1 mm yr^{-1} (Cazenave and Cozannet, 2014); 3.2 ± 0.4 mm yr^{-1} (Masters et al., 2012)] than during the 20th century [1.7 ± 0.2 mm yr^{-1} (Church et al., 2011; Ray and Douglas, 2011); 1.9 ± 0.3 mm yr^{-1} (Jevrejeva et al., 2014); 1.2 ± 0.2 mm yr^{-1} (Hay et al., 2015; Dangendorf et al., 2017)]. The dynamical response of the ocean and the atmosphere to climate variability as well as the glacier and ice-sheet water redistribution into the ocean and the terrestrial water storage, significantly contribute to sea level variability on interannual to longer time scales, and also to the spatial heterogeneity of sea-level rise (Church et al., 2013). In the Western Tropical Pacific, sea level has risen up to three times more than the global mean from the early 1990s (Cazenave and Cozannet, 2014). This rate (~7 mm yr^{-1}) is more than twice the rate observed from 1950 over the same region (~3 mm yr^{-1}) (Nerem et al., 2011; Becker et al. 2012). The opposite occurred in the Eastern Tropical Pacific, where sea level has increased at lower rates than the global mean from 1950 [~1 mm/year (Becker et al., 2012)] and declined during the 1993-2008 period [~ -3 mm yr^{-1} (Moon et al., 2013)]. This longitudinal trend gradient has been attributed to the effect of global warming and the acceleration of the trade winds (Timmermann et al., 2010; Merrifield, 2011; Becker et al., 2012; McGregor et al., 2012; Palanisamy et al., 2015), which has been related to climate variability at interannual-to-decadal scales driven by El Niño Southern Oscillation (ENSO, Church et al., 2011; Becker et al., 2012; Barnard et al., 2015) and the Pacific Decadal Oscillation (PDO, Merrifield et al., 2012; Zhang and Church, 2012; Han et al., 2013; Hamlington et al., 2014; Han et al., 2017). The role of the Atlantic multidecadal variability in the intensification of the Pacific trade winds has also been recently demonstrated (McGregor et al., 2014; Li et al., 2016; Sun et al., 2017 and references herein), although it is difficult to robustly quantify the contribution of the low-frequency climate oscillations to the tropical Pacific sea level trends due to the absence of longer tide gauge records.

A crucial factor which has often been overlooked and can considerably exacerbate the sea-level change impact at the coast is the vertical land motion (VLM) (Wöppelmann and Marcos, 2016). VLM, caused by natural processes, such as the Glacial Isostatic Adjustment (GIA), tectonics, volcanism and sediment compaction, or by human activities like, for instance, subsurface mineral and water extraction, can produce relative sea-level changes of the same order of magnitude as those caused by climate change and/or climate variability, and can

therefore give rise to major differences between local and regional sea-level rise (Wöppelmann and Marcos, 2016 and references herein). Here, we define the relative sea level (RSL) as the change in sea level relative to land, i.e. absolute (or geocentric) sea-level change minus local uplift or subsidence. Vertical land motion has been recognized, in many cases, as the main contributor to the RSL changes in the Southern Tropical Pacific, in particular the local vertical land motion caused by other processes than the GIA (Pfeffer et al., 2017 and references herein). Indeed, GIA only produces slight uplifts of about ~0.2 mm/year over our region of interest (Peltier et al. 2015). Accounting for the contribution of vertical land motion is particularly relevant in the South Western Tropical Pacific, one of the most tectonically active regions of the globe. In the region, the convergence between the Australian and Pacific plates is accommodated by several subduction zones (mainly the Solomon and New Hebrides ones where the Australian plate subducts towards the East and the Tonga-Kermadec subduction zone where the Pacific Plate subducts towards the West) and a complex deforming system (the North Fiji Basin) between these subductions (e.g. Pelletier et al., 1998). Plates are mainly rigid and their relative motion is accommodated by elastic deformation near plate borders: vertical movements may be slow when induced by the stress accumulation between earthquakes and sudden when the stress is released through earthquakes. Vertical movements can be up or down with variable amplitude depending on the magnitude of the earthquake and the position with respect to the rupture plane. For example, in the Torres Islands (southwest Pacific Archipelago of Vanuatu) where the Australian plate subducts beneath the North Fiji Basin, a sudden earthquake-related subsidence followed by slow interseismic coastal subsidence over the 1997-2009 period (~9 mm/year) together with an absolute (geocentric) regional sea-level rise resulted in a very high rate of relative sea-level change (~20 mm/year) and subsequent coastal inundation of inhabited low-lying areas (Ballu et al., 2011). Other examples of sudden vertical land motion related to the same subduction context are, for instance, on Malakula Island (Vanuatu), where a 1965 event led to 120 cm of abrupt coastal uplift (Taylor et al., 1980), and in the Solomon Archipelago, where a major M8.1 earthquake in 2007 caused more than 2 m of uplift in Ranongga Island and 1 m of subsidence on Simbo Island (Taylor et al., 2008; Saunders et al., 2015). Away from tectonic plate boundaries, in the central part of the Southern Tropical Pacific, tectonic activity is not likely to contribute significantly to vertical motions. However, this region is characterized by a high volcanism concentration (McNutt and Fischer, 1987; Adam et al., 2014), with slower vertical land motion than that occurring near plate boundaries (Nunn, 2009; Becker et al., 2012). One

example is Tahiti Island (French Polynesia), where a subsidence of ~0.5 mm/year is indicated by independent geodetic methods (Fadil et al., 2011; Becker et al., 2012).

Despite the high uncertainties of sea-level rise projections mainly associated with the unknowns of the processes driving the Antarctica and Greenland ice-sheets melting and shrinking (Church et al., 2013; Bamber and Aspinall, 2013; Ritz et al., 2015; DeConto and Pollard, 2016; Jevrejeva et al., 2016; Kopp et al., 2017), it is expected that global sea level rates continue increasing during the 21st century, especially at the Western Tropical Pacific where the highest sea-level rises are predicted (Church et el., 2013; Cazenave and Le Cozannet 2014; Kopp et al., 2014; Slangen et al., 2014; Carson et al., 2015; Jevrejeva et al., 2016). In such a context, coastal impacts assessment and adaptation planning critically need data on future sea level scenarios at the local scale (Church et al., 2013; Nicholls et al., 2014). Most of the previous studies, although they focused on relative sea level projections at the Southern Pacific, only included the VLM caused by the GIA (Church et el., 2013; Cazenave and Le Cozannet 2014; Kopp et al., 2014; Slangen et al., 2014; Carson et al., 2015; Jevrejeva et al., 2016). Considering the additional contribution of vertical land motion caused by other processes to relative sea level trends is therefore of high importance, as highlighted in The Fifth Assessment Report of the Intergovernmental Panel on Climate Change (AR5 IPCC) (Church et el., 2013). Some studies have investigated local vertical land motion at the small islands of the Southern Tropical Pacific (Nerem and Mitchum, 2002; Aung et al., 2009; Fadil et al., 2011; Becker et al., 2012; Ballu et al., 2014; Saunders et al., 2016; Pfeffer and Allemand, 2016; Pfeffer et al., 2017). However, these studies have one or more of the following limitations: i) the focus is on specific islands or archipelagos; ii) the uncertainty associated with the vertical land motion estimates obtained from different geodetic products is not explicitly estimated; iii) the quality of the data used to include VLM estimates into protections of future RSL is not properly assessed.

Here we present new estimates of relative sea-level changes at small islands of the South Western Tropical Pacific, and attempt to identify the contribution of local vertical land motion on these trends. This leads us to discuss the need, in the aim of establishing more robust future RSL projections, for a detailed analysis of the nature of the vertical land motion. We also attempt to overcome the above limitations by: i) using the most updated data available over the domain of interest from tide gauges, satellite radar altimetry and Global Positioning System (GPS) stations; ii) providing a measure of the vertical land motion uncertainty by including those associated with various satellite altimetry and GPS products; and iii) assessing the ability of the vertical land motion estimates to be projected into the future by examining

the time series in the past, especially paying attention to the tectonic context and the presence of earthquakes. Finally, we propose tentative future projections of relative sea level at a group of selected islands under three different greenhouse gases (GHG) emission scenarios (RCP2.6, RCP4.5 and RCP8.5) by combining the projected vertical land motion rates with the regionalized sea level projections presented in the AR5 IPCC (Church et al., 2013).

2. Data sets

2.1 Tide gauges and reconstructed Global Mean Sea Level

Tide gauge (TG) records are the main source of information on coastal sea-level changes since the mid-19th century. The TGs were engineered to measure the relative sea level, that is, the sea level relative to the land on which they are installed (Pugh, 1991). In this work, RSL records of an initial set of 35 TG stations located within the study domain (Fig. 1) and covering a minimum period of 4 years were obtained from the Permanent Service for Mean Sea Level (PSMSL; www.psmsl.org/data/obtaining/) at monthly scale and from both the University of Hawaii Sea Level Center (UHSLC; uhslc.soest.hawaii.edu) and the Système d'Observation du Niveau des Eaux Littorales (SONEL; www.sonel.org) at a daily scale. Monthly averaged values were calculated from daily values following the procedure detailed by the PSMSL (only months containing more than 15 valid days were considered, Holgate et al. 2013). Gaps in daily data are not filled before averaging into monthly means. Comments on the data quality provided by the PSMSL were all taken into account and no suspicious records were found. Concatenated sea level time series were produced for TG records provided by the same database and located at a maximum distance of 4 km, namely Funafuti (A and B), Honiara (A and B) and Rarotonga (A and B) from the UHSLC and Nauru and Nauru B from the PSMSL. Concatenation between two series was done ensuring that the mean of the sea level records were equal after removing the datum offset (bias) calculated over their overlapping periods with at least 6-month of time span and a minimum correlation coefficient of 0.95. Variance consistency between concatenated time series was confirmed by visual inspection. We finally selected the longest and most updated monthly time series at each location from a set including both concatenated and original records leading to a final subset of 27 records of which 5 were concatenated (see Table 1). We have also used the 1880-2013 Global Mean Sea Level (GMSL) monthly time series from the Church and White (2011) global sea level reconstruction (http://www.cmar.csiro.au/sealevel/sl_data_cmar.htm)

Table 1. Tide gauge, database, country, location, period of operation and percentage of gaps. Concatenated tide gauge records (see text) are marked with an asterisk. Closest GPS station to the tide gauge, distance to the closest tide gauge, coordinates and covered period for each GPS record obtained from SONEL and Nevada Geodetic Laboratory (NGL) databases.

Tide gauge							GPS					
Name	Database	Country	Lon (ºE)	Lat (ºN)	Total period	% Gaps	Closest GPS	Dist. (Km)	Lon (ºE)	Lat (ºN)	Period SONEL	Period NGL
Anewa Bay	UHSLC	Papua NG	155.88	-6.18	1968-1977	11	-	-	-	-	-	-
Honiara*	UHSLC	Solomon Is	159.95	-9.43	1974-2015	4	SOLO	0.5	159.96	-9.43	2008-2013	-
Noumea A	UHSLC	N Caledonia	166.44	-22.29	1967-2015	2	NOUM	3.8	166.41	-22.24	1997-2007	1997-2007
Ouinne	SONEL	N Caledonia	166.68	-21.98	1981-2015	85	YATE	33.8	166.94	-22.16	-	2008-2016
Nauru*	PSMSL	Nauru	166.9	-0.53	1974-2014	7	NAUR	3.7	166.93	-0.55	2003-2014	2003-2016
Lifou	SONEL	N Caledonia	167.28	-20.92	2011-2015	17	LPIL	1.7	167.26	-20.92	1996-2013	1996-2016
Norfolk Is	PSMSL	Australia	167.95	-29.07	1994-2014	4	NORF	2.2	167.94	-29.06	2008-2013	2008-2016
Port Vila VU A	UHSLC	Vanuatu	168.28	-17.75	1977-1982	6	-	-	-	-	-	-
Port Vila VU B	UHSLC	Vanuatu	168.28	-17.75	1993-2015	5	VANU	3.8	168.32	-17.76	2002-2013	2002-2013
Lautoka	PSMSL	Fiji	177.44	-17.6	1992-2014	0	LAUT	1	177.45	-17.61	2001-2013	2001-2016
Suva	PSMSL	Fiji	178.42	-18.14	1972-2015	6	SUVA	0.7	178.43	-18.14	1998-2002	1998-2002
"	"	"	"	"	"	"	FTNA	564.8	-178.12	-14.3	1998-2013	1998-2016
Funafuti*	UHSLC	Tuvalu	179.2	-8.53	1977-2015	3	TUVA	2.5	179.2	-8.5	2001-2013	2001-2016
Nukualofa	PSMSL	Tonga	-175.18	-21.14	1993-2014	1	TONG	0.3	-175.18	-21.14	2002-2013	-
Apia_A	UHSLC	Samoa	-171.75	-13.82	1954-1971	4	-	-	-	-	-	-
Apia_B	UHSLC	Samoa	-171.75	-13.82	1993-2015	3	SAMO	3.8	-171.74	-13.85	-	2001-2016
Kanton Is*	PSMSL	Kiribati	-171.72	-2.82	1949-2012	14	TUVA	1187.9	179.2	-8.5	2001-2013	2001-2016
Pago Pago	UHSLC	USA	-170.69	-14.28	1948-2014	3	ASPA	6.4	-170.72	-14.28	2001-2013	2001-2016
Rarotonga*	UHSLC	Cook Is	-159.78	-21.2	1977-2015	2	CKIS	1.9	-159.8	-21.2	2001-2013	2001-2016
Penrhyn	UHSLC	Cook Is	-158.07	-9.02	1977-2015	6	CKIS	1367.6	-159.8	-21.2	2001-2013	2001-2016
Papeete	UHSLC	F Polynesia	-149.57	-17.53	1969-2014	2	PAPE	0.4	-149.6	-17.5	2004-2013	2004-2016
"	"	"	"	"	"	"	THTI	3.9	-149.6	-17.5	1998-2013	-
Matavai	UHSLC	F Polynesia	-149.52	-17.52	1958-1967	32	-	-	-	-	-	-
Tubuai	SONEL	F Polynesia	-149.48	-23.34	2009-2013	13	TBTG	0.5	-149.48	-23.34	2009-2013	2009-2014
Rangiroa	SONEL	F Polynesia	-147.71	-14.95	2009-2014	31	-	-	-	-	-	-
Nuku Hiva	UHSLC	F Polynesia	-140.1	-8.92	1982-2015	34	-	-	-	-	-	-
Hiva Oa_A	UHSLC	F Polynesia	-139.03	-9.82	1977-1980	31	-	-	-	-	-	-
Hiva Oa_B	UHSLC	F Polynesia	-139.03	-9.82	2010-2015	25	-	-	-	-	-	-
Rikitea	UHSLC	F Polynesia	-134.97	-23.13	1969-2015	7	GAMB	0.9	-134.96	-23.12	2000-2010	2000-2016

2.2 Satellite Altimetry

Gridded monthly Sea Level Anomaly (SLA) during 1993-2015 was obtained from two different sources, namely AVISO (Archiving, Validation and Interpretation of Satellite Oceanographic data, http://www.aviso.altimetry.fr.) and CSIRO (Commonwealth Scientific and Industrial Research Organization; www.cmar. csiro.au/sealevel/sl_data_cmar.html). These two Sea Level Anomaly products were selected with the concern of having an assessment of the uncertainty. This choice was based on results from a previous study in which the AVISO (CSIRO) product scored the best (worst) product in terms of statistical uncertainty to be used for the calculation of vertical land motion by combining altimetry with

TGs at a global scale (Wöppelmann and Marcos, 2016). The two Sea Level Anomaly datasets consist of merged multi-missions data (TOPEX/Poseidon, Jason-1, Jason-2) spanning the period 1993-2015. The spatial resolution for the CSIRO dataset is of 1º x 1º and for the AVISO it is of 1/4º x 1/4º. The higher resolution of AVISO product primarily stems from accounting for other complementary missions (ERS- 1, ERS-2, Envisat, Geosat Follow-On, CryoSat, SARAL/AltiKa and Sentinel-3A/B). We linearly interpolated the CSIRO data on the 1/4º x 1/4º AVISO grid of higher resolution for comparison with tide gauge data. In addition, the effect of atmospheric pressure and wind on sea level is corrected for the AVISO dataset, whereas the TG records and CSIRO dataset includes these effects. For the sake of consistency in terms of signal contents across the sea level datasets, we added back the Dynamic Atmospheric Correction (DAC; Volkov et al., 2007), supplied by AVISO and containing these corrections, to the AVISO Sea Level Anomaly gridded product. A GMSL time series was computed by globally averaging the de-seasoned monthly Sea Level Anomaly from both data sets over 1993-2015.

2.3 Sea level projections

We used the Intergovernmental Panel on Climate Change's (IPCC) Fifth Assessment Report (AR5) projected global sea-level rise by 2100, forced by different GHG emission scenarios (IPCC, 2013). Projected sea-level rise under each scenario is the sum of individual contributions from steric changes and melting of glaciers and ice caps, the Greenland Ice Sheet, the Antarctic Ice Sheet, and land water storage (CMIP5, Taylor et al. 2012). We considered three representative concentration pathways (RCP) scenarios ranging from drastic emission reductions (RCP 2.6) to moderate (RCP 4.5) and unmitigated growth of emissions (RCP 8.5). These data sets are obtained from the Integrated Climate data Center of the University of Hamburg (ICDC, http://icdc.cen.uni-hamburg.de/1/daten/ocean/ar5-slr.html). These datasets consist of gridded fields of projected sea-level change calculated as the 20-yr mean differences between the 2081-2100 and the 1986-2005 periods, with a spatial resolution of 1º x 1º, for 9 geophysical components driving long-term sea-level changes including the dynamic sea surface height, the thermosteric and the inverse barometer effect (see Fig. S1). We linearly interpolated the set of sea level projected fields to the 1/4º x 1/4º AVISO grid for comparison (see Fig. S1).

2.4 GPS

The linear trend estimates of vertical land motion derived from GPS data (VLM_{GPS}) of 18 stations located within the study domain were obtained from two different datasets produced by Système de l'Observation du Niveau des Eaux Littorales (SONEL, ULR6 velocity field, Santamaria-Gomez et al., 2017, http://www.sonel.org/-GPS-.html) and Nevada Geodetic Laboratory (NGL, IGS08-MIDAS velocity field,Blewitt et al., 2016, http://geodesy.unr.edu/velocities/midas.IGS08.txt) (see Table 1). These two data sets were selected because they use rather different methods and strategies to analyze the GPS measurements and estimate linear trends of the station positions. VLM_{GPS} trend estimates from SONEL are derived from daily station position time series obtained by using a combination of manual and automatized procedures to detect and remove offsets produced by natural processes (e.g., earthquakes) and/or instrumentation artefacts (changes or malfunctioning of GPS equipment) that can bias the estimation of the underlying linear trends of station positions (Gazeaux et al., 2013). The NGL linear trend estimates result from a different and automatized method which is claimed to be robust regarding offsets (Blewitt et al., 2016). Details are given on the websites of each dataset and can be found in the publications. These methodological differences have the potential to lead to significant differences in the VLM_{GPS} estimates and also in its uncertainties (Gazeaux et al., 2013; Rebischung et al., 2016). But they represent the state-of-the art in GPS data analysis, and the differences in their estimates can provide a better appraisal of the real uncertainties beyond the statistical ones. Both VLM_{GPS} estimates and associated station position time series were obtained from SONEL (http://www.sonel.org/-GPS-.html) and NGL (http://geodesy.unr.edu/NGLStationPages/GlobalStationList) websites, respectively. These time series were examined to detect offsets or post-seismic deformation due to the occurrence of earthquakes. The nearest GPS station to each tide gauge station was searched and selected. When two or more GPS stations where similarly close to a TG station, the longest one (taking into account the gaps) was then selected, with the exception of the tide gauge of Papeete where the two closest GPS stations (PAPE and THTI) were finally selected (in spite of THTI being longer than PAPE) because they showed opposite VLM trends.

2.5 GIA

We used outputs of the GIA model ICE-6G (VM5a) (Peltier et al, 2015, http://www.atmosp.physics.utoronto.ca/~peltier/data.php) consisting of gridded fields with a spatial resolution of 1/5º x 1/5º of the two GIA components driving relative sea-level changes,

one accounting for its effect on the vertical crustal motion (VLM_{GIA}) and another accounting for its effect on the sea surface height due to changes in gravity ($GEOID_{GIA}$) (Tamisiea and Mitrovica, 2011). The net GIA effect on relative sea-level changes (NET_{GIA}) is the combination of these two effects and it can be defined as $NET_{GIA} = GEOID_{GIA} - VLM_{GIA}$. We linearly interpolated the GIA dataset to the 1/4º x 1/4º AVISO grid for comparison.

3. Methodology

3.1 Relative sea level trends from tide gauges

Relative sea level trends (RSL_{TG}) were calculated by least squares linear fitting from the TG records over their total period and over the 1993-2015 period for comparison with the altimetric data (when both periods overlapped a minimum of 75% of the time) (see Table 1). The time series were previously deseasoned by removing the climatological monthly mean from the monthly values. Incomplete years were removed before computing the climatological monthly means. Uncertainties were defined as the Standard Error (SE) of the fit adjusted for lag-1 autocorrelation (Santer et al., 2000). One study found this method appropriate for annual RSL data but not recommendable for monthly data because the trend uncertainty may be underestimated (Bos et al., 2014). However, a recent global analysis of the PSMSL tide gauges (Pfeffer et al., 2016) found no significant differences in the SE adjusted by this method between monthly and annual data in agreement with a similar analysis that we performed with the TG records in this study (Table S1).

3.2 Vertical land movements

In addition to VLM estimates from GPS, VLM can be obtained by subtracting TG data from satellite radar altimetry data (VLM_{ATG}). Indeed, as sea levels from satellite altimetry are expressed relative to the Earth's centre of mass and those from TGs are relative to the land surface, the difference corresponds to a quantity similar to a geocentric vertical land surface motion, provided that the instrumental drifts are negligible and the oceanic signal content in both sea level measurements is identical (Cazenave et al., 1999). In this study, two sources of satellite altimetry data were considered (section 2), hence two different ATG monthly time series were produced at each TG location. Note that the satellite altimetry time series correspond to the spatially averaged Sea Level Anomaly time series over a region of 0.5 degree of radius around the corresponding closest grid to each TG. Also note that a minimum of 70% of common sea level period was necessary to compute the above-mentioned differences between satellite and tide gauge data. Subsequently, two estimates of vertical land

motion were obtained by calculating the least squares linear trends (VLM_{ATG}) from the ATG monthly time series over the 1993-2015 period. SE of the fit were adjusted for lag-1 autocorrelation (Santer et al., 2000). A combined estimate of the VLM_{ATG} trends was computed at TG locations by averaging the two VLM_{ATG} trend values obtained from each of the altimetry datasets (AVISO and CSIRO) weighted by their respective inverse squared uncertainty. Similarly, a combined estimate of the VLM_{GPS} trend was computed at each location by averaging the two different VLM_{GPS} trend values obtained from SONEL and NGL weighted by their respective inverse squared uncertainty. Uncertainties were estimated using the standard error of a weighted mean.

The RSL variations at the TG locations were compared with GMSL, by estimating the linear trend of the difference between the TG records to both the satellite altimetry Global Mean Sea Level (1993-2015, Table 1 and Fig. 1a) and the reconstructed GMSL (1880-2013, Table 1 and Fig. 1b, Church et al. 2013) during their overlapping period. Only differenced time series covering at least five years were used to calculate the trends (Table 2).

3.3 Estimation of future changes of relative sea level

For the calculation of the projected RSL changes over the twenty-first century and their corresponding uncertainties, we first obtained estimates of the projected absolute sea-level (PSL) changes by combining all the geophysical components described in section 2.1.3 (see Church et al., 2013b for more details). We then calculated projections of vertical land motion due to GIA (VLM_{GIA}), which is the only geophysical process for which there are reasonably accurate models available, and due to any vertical land motion process (VLM_{TOTAL}) as observed by satellite techniques, provided there was no-evidence of past non-linearity in the time series (e.g., due to earthquakes). Projections of RSL ($PRSL_{GIA}$ and $PRSL_{TOTAL}$) at these selected locations were finally obtained by subtracting either VLM_{GIA} or VLM_{TOTAL} (VLM_{ATG} and VLM_{GPS}) projections to the projected absolute sea-level projections at their closest grid points and finally adding the $GEOID_{GIA}$ projections to account for the geoid effect of GIA.

$$PRSL_{GIA} = PSL - VLM_{GIA} + GEOID_{GIA} = PSL + NET_{GIA} \quad (1)$$

$$PRSL_{TOTAL} = PSL - VLM_{TOTAL} + GEOID_{GIA} \quad (2)$$

Standard errors for the projections were calculated as the root-sum-square of standard errors in PSL and vertical land motion projections.

4. Results

The spatial pattern of absolute sea level (ASL) trends from AVISO (1993-2015) is shown in Figure 1a. Significant trends were found overall in the study domain and higher values than the absolute Global Mean Sea Level rate (2.9 ± 0.1 mm yr^{-1}) were found over the region covering the central and north western parts of the domain (~5 mm yr^{-1} on average and maximum values of 9.0 ± 1.3 mm yr^{-1}). Lower rates than global were found over the region covering the south western and eastern parts of the domain (~ 2 mm yr^{-1} on average and minimum values of 1.0 ± 0.5 mm yr^{-1}).

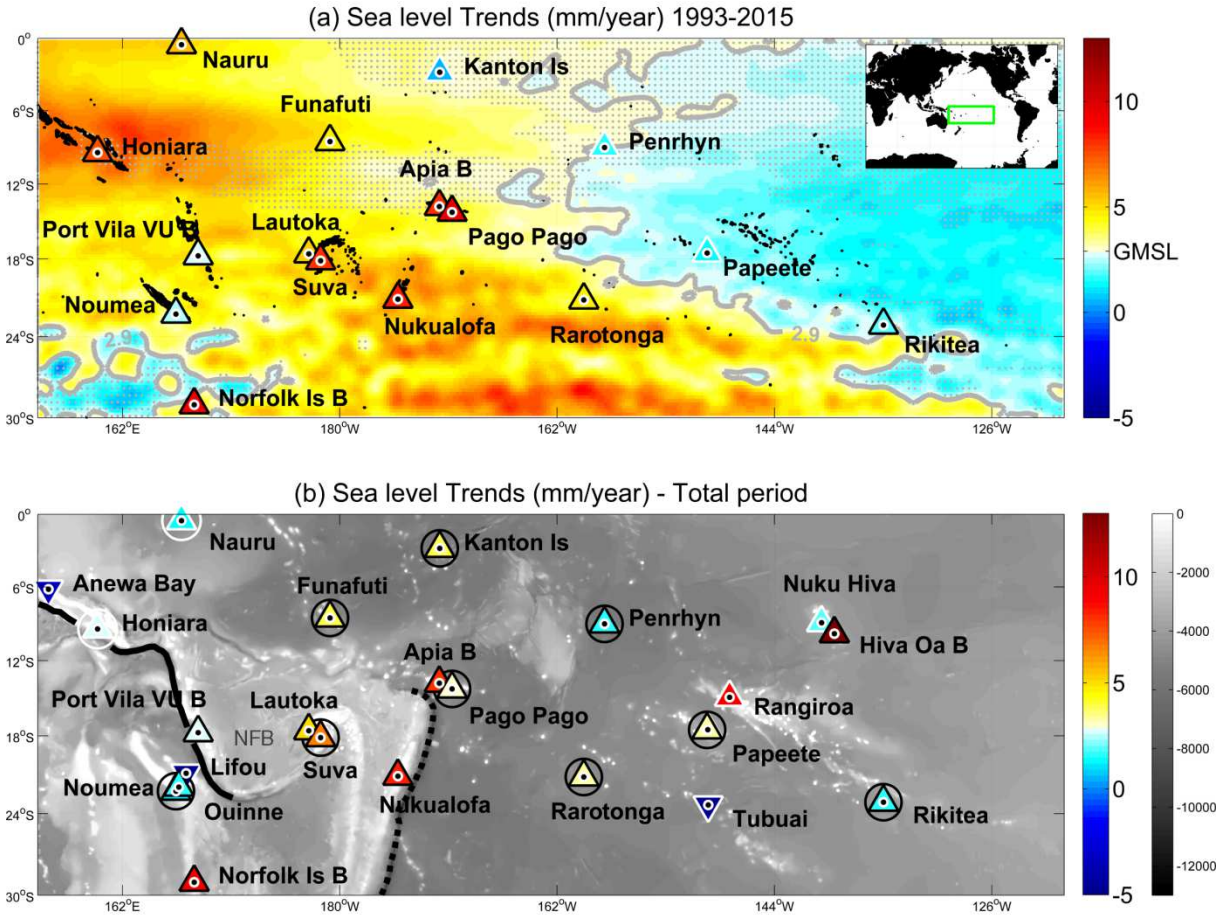

Figure 1. Relative Sea level trends (mm/year) at tide gauges (coloured triangles) and absolute sea level trends at AVISO altimetry grid points (coloured areas) calculated over the 1993-2015 period (a) and over the total period of each tide gauge (b). Grey contours mark global

mean sea level trend during 1993-2015. White-bordered triangles (a,b) and dot-shaded areas (a) denote no statistical significance at the 2σ confidence level. Black circles denote tide gauges records longer than 40 years. Note that the colorbar is designed to emphasize the difference between sea level trends and the GMSL, but values are strictly sea level trends. GEBCO_2014 (Weatherall et al. 2015) bathymetry (in meters) is also shown (b) to highlight tectonic features in the region. The Eastward dipping Solomon and New Hebrides subduction zones are evidenced by the elongated trench running long Anewa Bay, Honiara and Port-Vila (continuous black line) and the Westward dipping Tonga-Kermadec subduction zone runs East of Nukualofa (dashed black line). The North Fiji Basin (NFB on the map), North-West of Suva and Lautoka is shallower than the Pacific plate to the East and displays many tectonic features.

Even though RSLs from TGs can be expected to depart from the GMSL for various reasons, Figure 1b intentionally displays them to highlight these differences. Significant trends of RSL were found in most of the longest tide gauge records, with time spans ranging from 40 to 66 years (Table 1 and Fig 1b). Trend values significantly higher than the absolute GMSL were found at most of the tide gauges located over the central part of the domain (-170ºW to 170ºE) ranging from 2.9 ± 0.5 mm yr^{-1} (0.8 mm yr^{-1} higher than GMSL) at Pago Pago to 6.6 ± 0.7 mm yr^{-1} (4.2 mm yr^{-1} higher than GMSL) at Suva. Lower but still significant trends were found at most of the stations located at the western and eastern parts of the domain. Trends significantly lower than the GMSL were found at two stations, namely Noumea (0.9 ± 0.4 mm yr^{-1} [-1.4 mm yr^{-1} lower than GMSL]) and Rikitea (1.7 ± 0.3 mm yr^{-1} [-0.6 mm yr^{-1} lower than GMSL]) (Table 2 and Fig. 1b). Non-significant differences between TG and GMSL trends were found at two of the longest tide gauge records, namely Funafuti (3.8 ± 1.3 mm yr^{-1}) and Honiara (2.8 ± 1.9 mm yr^{-1}), located in the region where sea level has a large interannual variability associated with ENSO resulting in large uncertainties in sea level trends (Church et al., 2006, Becker et al. 2012). The corresponding deviations of the ASL trends with respect to the global sea-level rise are thought to result from the climate variability driving regional sea-level changes from interannual to multidecadal scales, while differences between TG and GMSL trends are assumed to be due to climate variability, record length, VLM, instrumental errors or a combination of all. They will be discussed as appropriate later on.

Table 2. Relative sea level trends at tide gauge stations calculated over both the total period and 1993-2015. Trends of the difference between the TG records to both the satellite altimetry GMSL (1993-2015, common period) and the reconstructed GMSL (total period) over their overlapping period (in parenthesis). Asterisks denote tide gauge records longer than 40 years. Absolute sea level trends at the closest grid points to the tide gauge locations and their differences with respect the Global Mean Sea Level. Trends of the differenced time series of

monthly satellite altimetry (AVISO and CSIRO products) minus tide gauge data, standard errors and their weighted means of the trends. VLM_{GPS} trends and standard errors (SONEL, NGL and their weighted means) at the closest GPS sites to the tide gauge stations. Non-robust vertical land motion estimates at GPS sites as considered by the GPS centers are denoted with the term *NR*. Total weighted means of vertical land motion trends and standard errors are also listed. Black bold values indicate statistical significance at 2σ level.

		Sea level Trends			Vertical land motion Trends								
		Total period	1993-2015 (common period)		VLM ATG (mm·yr-1)						VLM GPS (mm·yr-1)		
Tide gauge	Total period	RSL Trend (mm·yr-1)	RSL Trend (mm·yr-1)	ASL AVISO Trend (mm·yr-1)	AVISO	CSIRO	Weighted mean	Closest GPS	Period SONEL	Period NGL	SONEL	NGL	Weighted mean
Anewa Bay	1968-1977	-3.6 ± 13.7 (-6.0 ± 13.7)	- (-)	- (-)	-	-	-	-	-	-	-	-	
Honiara*	1974-2015	2.8 ± 1.9 (0.5 ± 2.1)	**7.6 ± 3.4** (4.8 ± 3.4)	**7.7 ± 3.5** (4.9 ± 3.5)	0.0 ± 0.3	**-1.3 ± 0.4**	-0.3 ± 0.2	SOLO	2008-2013	-	*NR*	-	-
Noumea A*	1967-2015	**0.9 ± 0.4 (-1.4 ± 0.4)**	**2.4 ± 1.0** (-0.4 ± 1.0)	**4.2 ± 0.8** (1.4 ± 0.8)	**1.7 ± 0.3**	**1.6 ± 0.4**	**1.7 ± 0.2**	NOUM	1997-2007	1997-2007	**-1.4 ± 0.3**	-2.0 ± 1.2	**-1.4 ± 0.3**
Ouinne	1981-2015	**1.7 ± 0.3** (-1.4 ± 5.1)	- (-)	- (-)	-	-	-	YATE	-	2008-2016	-	1.7 ± 1.7	1.7 ± 1.7
Nauru*	1974-2014	1.4 ± 1.0 (-1.6 ± 0.9)	**5.5 ± 2.5** (2.7 ± 2.5)	**5.3 ± 2.1** (2.5 ± 2.1)	-0.2 ± 0.8	-1.1 ± 1.0	-0.6 ± 0.6	NAUR	2003-2014	2003-2016	**-1.0 ± 0.3**	-0.3 ± 1.0	**-0.9 ± 0.2**
Lifou	2011-2015	-5.0 ± 9.7 (-8.8 ± 9.7)	- (-)	- (-)	-	-	-	LPIL	1996-2013	1996-2016	0.2 ± 0.4	**-2.6 ± 1.2**	-0.2 ± 0.4
Norfolk Is	1994-2014	**9.3 ± 2.1 (6.5 ± 2.2)**	**9.3 ± 2.1 (6.5 ± 2.2)**	**2.6 ± 1.0** (-0.5 ± 1.0)	**-7.1 ± 2.2**	**-7.9 ± 1.9**	**-7.5 ± 1.4**	NORF	2008-2013	2008-2016	0.4 ± 0.4	-1.0 ± 0.8	0.1 ± 0.3
Port Vila VU A	1977-1982	13.6 ± 16.1 (-)	- (-)	- (-)	-	-	-	-	-	-	-	-	-
Port Vila VU B	1993-2015	**2.8 ± 1.3** (0.0 ± 1.4)	**2.8 ± 1.3** (0.0 ± 1.4)	**4.9 ± 1.0** (2.0 ± 1.0)	**1.8 ± 0.4**	**1.6 ± 0.5**	**1.7 ± 0.3**	VANU	2002-2013	2002-2013	*NR*	*NR*	-
Lautoka	1992-2014	**5.2 ± 1.5** (2.3 ± 1.5)	**5.2 ± 1.5** (2.3 ± 1.5)	**5.5 ± 1.3** (2.7 ± 1.3)	0.3 ± 0.3	0.3 ± 0.3	0.3 ± 0.2	LAUT	2001-2013	2001-2016	**-1.2 ± 0.3**	-0.6 ± 1.2	**-1.1 ± 0.3**
Suva*	1972-2015	**6.6 ± 0.7 (4.2 ± 0.7)**	**8.2 ± 1.6 (5.4 ± 1.7)**	**6.0 ± 1.3** (3.2 ± 1.3)	**-2.2 ± 0.5**	**-2.5 ± 0.6**	**-2.3 ± 0.4**	SUVA	1998-2002	1998-2002	*NR*	-4.0 ± 4.1	-4.0 ± 4.1
"	"	"	"	"	"	"	"	FTNA	1998-2013	1998-2016	-0.3 ± 0.3	-0.2 ± 2.3	-0.3 ± 0.3
Funafuti*	1977-2015	**3.8 ± 1.3** (1.0 ± 1.4)	**4.6 ± 2.1** (1.8 ± 2.1)	**4.9 ± 2.2** (2.1 ± 2.2)	**0.4 ± 0.2**	-0.4 ± 0.3	0.2 ± 0.2	TUVA	2001-2013	2001-2016	**-1.7 ± 0.2**	-1.7 ± 1.1	**-1.7 ± 0.2**
Nukualofa	1993-2014	**8.3 ± 1.1 (5.2 ± 1.2)**	**8.3 ± 1.1 (5.5 ± 1.2)**	**6.8 ± 1.1 (4.0 ± 1.1)**	**-1.5 ± 0.2**	**-2.1 ± 0.5**	**-1.6 ± 0.2**	TONG	2002-2013	-	**3.0 ± 0.4**	-	**3.0 ± 0.4**
Apia A	1954-1971	0.0 ± 1.6 (-1.1 ± 1.6)	- (-)	- (-)	-	-	-	-	-	-	-	-	-
Apia B	1993-2015	**8.2 ± 2.2 (5.3 ± 2.2)**	**8.2 ± 2.2 (5.3 ± 2.2)**	3.7 ± 2.2 (0.9 ± 2.2)	**-4.4 ± 0.7**	**-4.9 ± 0.7**	**-4.7 ± 0.5**	SAMO	-	2001-2016	-	**-5.0 ± 1.6**	**-5.0 ± 1.6**
Kanton Is*	1949-2012	**3.7 ± 0.5 (1.8 ± 0.6)**	0.4 ± 2.5 (-2.4 ± 2.5)	0.8 ± 2.9 (-2.0 ± 2.8)	0.2 ± 0.2	-0.1 ± 0.2	0.1 ± 0.1	TUVA	2001-2013	2001-2016	**-1.7 ± 0.2**	-1.7 ± 1.1	**-1.7 ± 0.2**
Pago Pago*	1948-2014	**2.9 ± 0.5 (0.8 ± 0.4)**	**9.5 ± 2.4 (6.7 ± 2.4)**	**4.0 ± 2.1** (1.2 ± 2.1)	**-5.5 ± 1.2**	**-6.4 ± 1.0**	**-6.1 ± 0.7**	ASPA	2001-2013	2001-2016	*NR*	**-5.4 ± 1.5**	**-5.4 ± 1.5**
Rarotonga*	1977-2015	**3.4 ± 0.5** (1.0 ± 0.6)	**4.6 ± 1.0** (1.8 ± 1.0)	**4.2 ± 1.0** (1.4 ± 1.0)	**-0.4 ± 0.2**	0.0 ± 0.6	-0.3 ± 0.2	CKIS	2001-2013	2001-2016	-0.5 ± 0.4	-0.1 ± 1.1	-0.5 ± 0.3
Penrhyn*	1977-2015	**1.7 ± 0.8** (-1.2 ± 0.9)	1.5 ± 1.7 (-1.3 ± 1.6)	2.4 ± 1.7 (0.4 ± 1.6)	**0.8 ± 0.2**	0.3 ± 0.4	**0.7 ± 0.2**	CKIS	2001-2013	2001-2016	-0.5 ± 0.4	-0.1 ± 1.1	-0.5 ± 0.3
Papeete*	1969-2014	**3.2 ± 0.4** (0.9 ± 0.5)	1.3 ± 1.0 (-1.4 ± 1.0)	**1.5 ± 0.9** (-1.3 ± 0.9)	0.1 ± 0.2	-0.2 ± 0.3	0.1 ± 0.1	PAPE	2004-2013	2004-2016	**-1.9 ± 0.2**	-1.5 ± 1.2	**-1.9 ± 0.2**
"	"	"	"	"	"	"	"	THTI	1998-2013	-	**-0.5 ± 0.2**	-	**-0.5 ± 0.2**
Matavai	1958-1967	2.1 ± 2.0 (2.2 ± 2.3)	- (-)	- (-)	-	-	-	-	-	-	-	-	-
Tubuai	2009-2013	-9.4 ± 15.1 (-12.7 ± 15.3)	- (-)	- (-)	-	-	-	TBTG	2009-2013	2009-2014	-0.3 ± 0.5	-1.6 ± 1.2	-0.5 ± 0.5
Rangiroa	2009-2014	9.1 ± 6.0 (6.0 ± 6.0)	- (-)	- (-)	-	-	-	-	-	-	-	-	-
Nuku Hiva	1982-2015	1.9 ± 1.3 (-1.4 ± 1.5)	- (-)	- (-)	-	-	-	-	-	-	-	-	-
Hiva Oa A	1977-1980	3.5 ± 8.9 (-)	- (-)	- (-)	-	-	-	-	-	-	-	-	-
Hiva Oa B	2010-2015	**39.8 ± 9.4** (-)	- (-)	- (-)	-	-	-	-	-	-	-	-	-
Rikitea*	1969-2015	**1.7 ± 0.3 (-0.6 ± 0.3)**	**1.8 ± 0.8** (-1.0 ± 0.8)	**1.7 ± 0.8** (-1.0 ± 0.8)	0.1 ± 0.2	-0.8 ± 0.5	-0.1 ± 0.2	GAMB	2000-2010	2000-2016	**-1.0 ± 0.4**	-0.9 ± 1.2	**-1.0 ± 0.4**

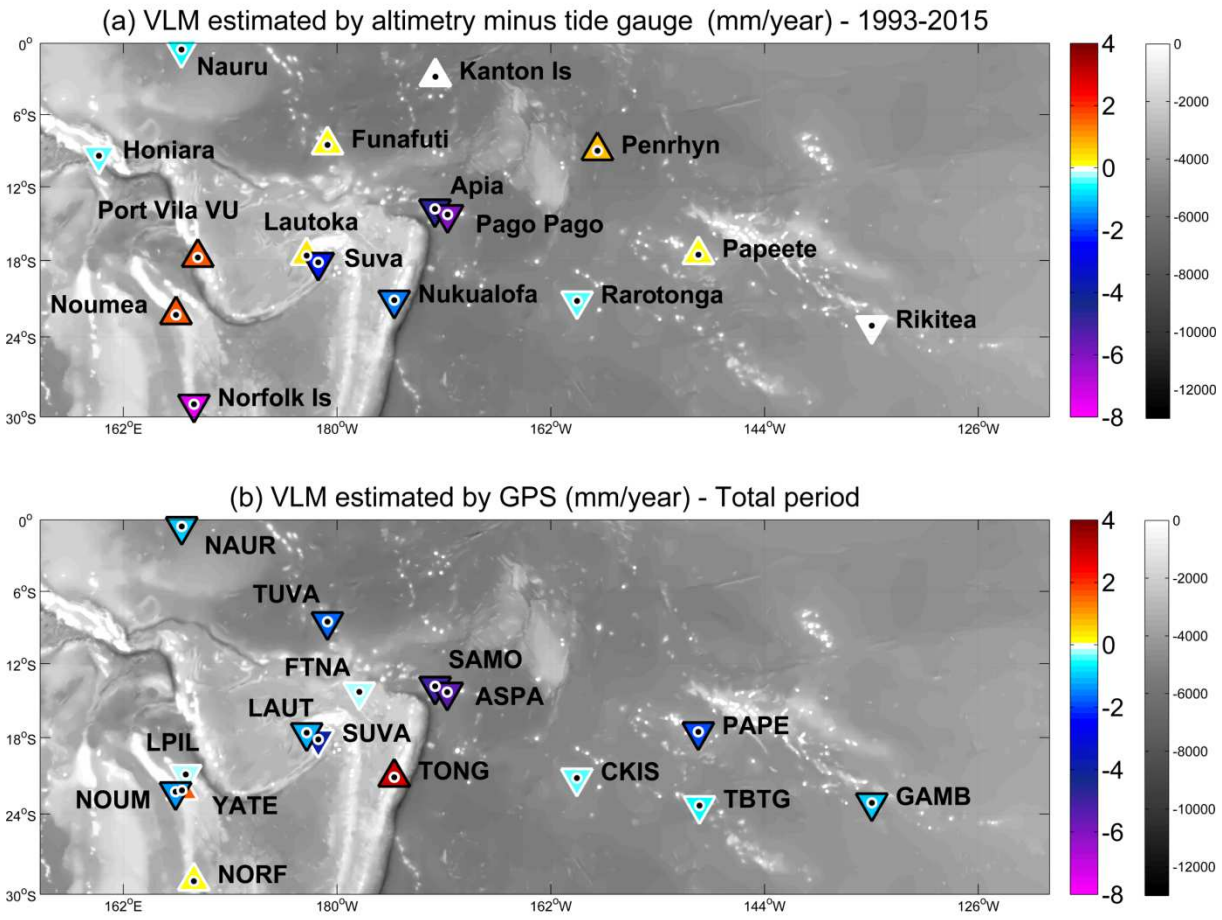

Figure 2. VLM_{ATG} weighted means (AVISO and CSIRO) calculated over 1993-2015 at the tide gauge locations (a) and VLM_{GPS} weighted means (SONEL and NGL) calculated at their closest GPS stations (b). Upward (downward) triangles denote positive (negative) VLM values. White-bordered triangles denote no statistical significance at 2σ level. GEBCO bathymetry (in meters) is also shown.

A comparison of ASL and RSL trends at each TG station over the altimetry period is shown in Figure 1a and listed in Table 2. The spatial pattern of the RSL trends obtained from tide gauge records was overall found very similar to that of the ASL trends from altimetry, with positive trends over all the domain and maximum values at the stations located at central and north western parts of the domain, namely Pago Pago (9.5 ± 2.4 mm yr^{-1} [6.7 mm yr^{-1} higher than GMSL]) and Honiara (7.6 ± 3.4 mm yr^{-1} [4.8 mm yr^{-1} higher than GMSL]) and minimum values at the tide gauges located at the south western and eastern parts, namely Rikitea (1.8 ± 0.8 mm yr^{-1} [-1.0 mm yr^{-1} lower than GMSL]) and Noumea A (2.4 ± 1.0 mm yr^{-1} [-0.4 mm yr^{-1} lower than GMSL]) (Table 2 and Figs. 1a, b).

However, locally significant differences between ASL and RSL trends were found at 8 out of the 27 tide gauge locations (Table 2). These differences can be due to VLM. For instance, significant subsidences were found in the central part of the domain at Pago Pago (-6.1 ± 0.7 mm yr^{-1}), Apia B (-4.7 ± 0.5 mm yr^{-1}), Suva (-2.3 ± 0.4 mm yr^{-1}) and Nukualofa (-1.6 ± 0.2 mm yr^{-1}), and the highest subsidence was found at Norfolk Island, which is located in the south western part (-7.5 ± 1.4 mm yr^{-1}) (Fig. 2a and Table 2). Significant uplift was found at three tide gauges: Port Vila B (1.7 ± 0.3 mm yr^{-1}), Noumea A (1.7 ± 0.2 mm yr^{-1}), and Penrhyn (0.7 ± 0.2 mm yr^{-1}). Note that the uplift obtained for the Port-Vila tide gauge (VLM_{ATG}) may be overestimated due to the fact that a ~11cm offset related to an earthquake in 2002 (Level, 2009) has been corrected in the tide gauge series available from the UHSLC website . Discrepancies between VLM_{ATG} from AVISO and CSIRO were found at two stations: first, at Honiara, where no significant vertical land motion was found with AVISO dataset, whereas a significant subsidence (-1.3 ± 0.4 mm yr^{-1}) was found with CSIRO; second, at Funafuti, where significant trends (at 2σ level) with opposite sign were found with AVISO (0.4 ± 0.2 mm yr^{-1}) and CSIRO (-0.4 ± 0.3 mm yr^{-1}) (Table 2 and Fig. 3a).

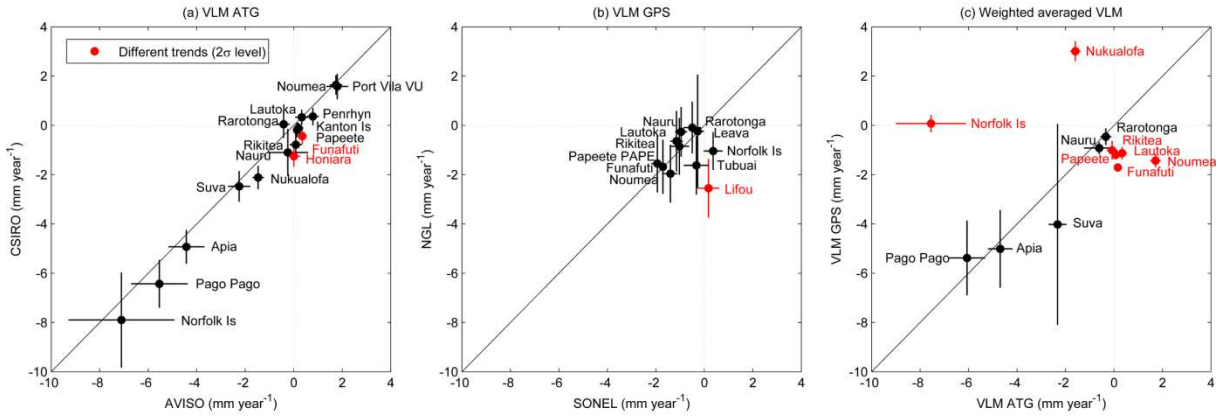

Figure 3. Scatterplot between trends of vertical land motion from (a) satellite radar altimetry minus tide gauge (VLM_{ATG}) data from AVISO and CSIRO, (b) GPS data from SONEL and NGL, and (c) weighted means of VLM_{ATG} and VLM_{GPS} trends (see section 3). Error bars denote one σ standard error. In red colour denotes that trends are different at the 2σ significance level (T-test).

A question now arises as to whether VLM trend estimates obtained by using different approaches are consistent with each other. To answer this question, we first compared the VLM_{ATG} with the VLM_{GPS} obtained from the GPS data centers. Significant subsidence (weighted averaged VLM_{GPS}) was found at 11 out of the 19 GPS stations, with the highest

values at those stations located over the central part of the domain: Pago Pago (ASPA, -5.4 ± 1.5 mm yr^{-1}) and Apia B (SAMO, -5.0 ± 1.6 mm yr^{-1}), which are affected by a major earthquake (Fig. 2b and Table 2), the 2009 M8.1 Samoa earthquake which occurred on the outer rise of the Tonga-Kermadec subduction zone. This earthquake is responsible for a significant sudden offset in the timeseries, but also a longer-term change in the ground motion due to post-seismic deformation. Such major seismic events are a real issue in terms of sea-level monitoring using tide gauges since their long-term impact (due to the post-earthquake viscoelastic deformation occurring in the lower crust and upper mantle (i.e. Johnson and Tebo, 2018)) cannot easily be modeled and accounted for. Lower but still significant subsidence was found at most of the remaining stations with values ranging from -0.9 ± 0.2 mm yr^{-1} at Nauru (NAUR) to -1.9 ± 0.2 mm yr^{-1} at Papeete (PAPE). Nukulaofa (TONG) is the only location where a significant VLM_{GPS} uplift (3.0 ± 0.4 mm yr^{-1}) was found. Note that VLM_{GPS} estimates shown for ASPA, SAMO and TONG are not weighted averages because they were considered non-robust by SONEL. Discrepancies between SONEL and NGL VLM_{GPS} were found only at Lifou (LPIL) where a high subsidence was found only for SONEL (Table 2 and Fig. 3b). Major discrepancies were found between VLM_{GPS} and VLM_{ATG} at 7 out of the 12 locations when weighted averaged trends were compared. In particular, significant VLM_{GPS} subsidence was found at five locations where the VLM_{ATG} were found either non-significant (Lautoka, Funafuti, Papeete and Rikitea), or positive, as in Noumea A in agreement with the VLM_{ATG} uplift of 2.5 ± 1.5 mm/yr found by Nerem and Mitchum (2002) (Table 2 and Fig. 3c). Significant VLM_{ATG} subsidence was found at two locations, namely Norfolk Island and Nukulaofa, where VLM_{GPS} were found non-significant and positive, respectively. These discrepancies were not present at 5 of these 7 stations (Lautoka, Funafuti, Nukulaofa, Papeete and Rikitea) when VLM_{ATG} estimates were directly compared with VLM_{GPS} estimates from NGL, mainly due to much higher uncertainties. Note that significant VLM_{GPS} subsidence was found at Papeete at two different GPS stations for SONEL, namely PAPE (-1.9 ± 0.2) and THTI (-0.5 ± 0.2), located very close to each other (1 and 3900 m from the tide gauge, respectively), indicating the high spatial variability of the VLM_{GPS} trend estimates at this island.

5. Discussion

We have investigated sea level trends at the islands located over the South Western Tropical Pacific region, both through their variation with respect to the land surface and through their geocentric variation. This has allowed us to identify (Fig. 1) and quantify (Fig. 2) the contribution of ground vertical movements to sea level trends observed at the coast using independent geodetic methods and assuming a linear rate of change. We have found that RSL rose at higher rates than the GMSL over the last 4-6 decades, especially where the highest land subsidence occurred, coinciding with the region where the Pacific and Australian tectonic Plates converge. Differences and similarities between local RSL trends and the GMSL rise (Fig. 1) can be at least partially accounted for by the presence or absence of VLM, as at Honiara, Noumea and Penrhyn, where the vertical displacements of the tide gauge with respect to the centre of mass of the Earth significantly accounted for these differences (Table 2 and Fig. S4).

At Noumea and Penrhyn, however, VLM_{ATG} and VLM_{GPS} estimates are not consistent, indicating probably that the TG is subject to non-linear processes, such as earthquakes, superimposed on the long-term motion detected at the GPS station. However, no evidence of earthquakes has been found at Penrhyn. At Nauru, Suva, Pago Pago and Rarotonga, we did not find discrepancies between VLM_{ATG} and VLM_{GPS} estimates although they cannot totally account for the long-term local sea level deviations with respect the GMSL trend. It might have been due either to the presence of non-linear VLM, or to the impact of multidecadal climate variability, which can produce at Pago Pago deviations of similar magnitude to the observed (Becker et al., 2012), or to a combination of both. TGs did not subside over the altimetry period at Funafuti, Kanton Island and Papeete, but they recorded a high sea-level rise over the long-term, in agreement with subsidence found at the GPS data. A possible explanation for this can be that non-linear uplifts occurred at the start of the altimetry period, which could not be registered at the GPS records. No evidence of earthquakes was found at Kanton Island and Papeete, which carries the implication of other processes, for instance related to the stability of the volcanic edifice or to the influence of multi-decadal regional variability which may be especially important at Funafuti and Papeete (Becker et al., 2012). It is worth mentioning that the complex behavior of the volcanic edifice at Tahiti may cause different rates of vertical land motion depending on the location (S. Calmant, personal communication). At Rikitea, RSL rose at a lower rate than globally on the long term, and it cannot be accounted for by any of the VLM estimates and neither by regional multidecadal

variability, which has an opposite effect on sea level trends at this location (Becker et al., 2012). We have no explanation for this discrepancy.

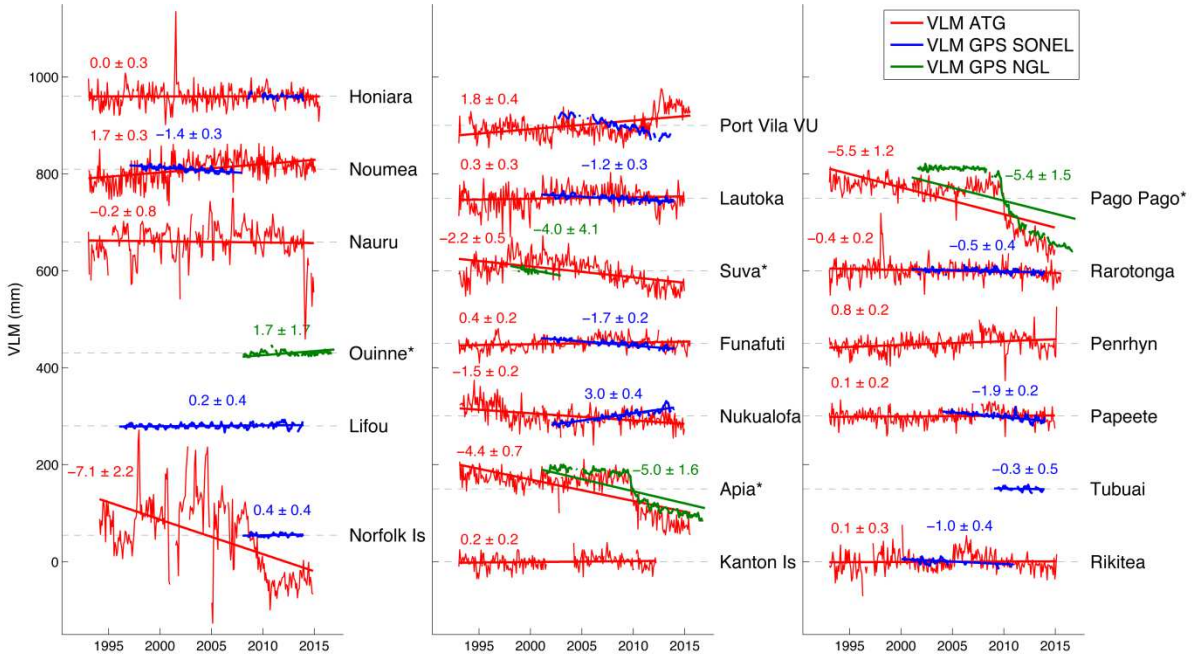

Figure 4. VLM_{ATG} time-series at tide gauge locations from the AVISO satellite altimetry database (red lines). VLM_{GPS} time-series from SONEL (blue lines) and from NGL (green lines). Units are millimetres. VLM_{ATG} ,VLM_{GPS} and standard error values are shown together with their corresponding linear trend lines (units in mm/year). Asterisks denote the locations where robust VLM_{GPS} trends from SONEL are not available and VLM_{GPS} time-series, in this case the trends from NGL are plotted. VLM_{GPS} values are absent at the locations where robust VLM_{GPS} estimates are not available for both SONEL and NGL.

We have explored the uncertainty associated with VLM at three different levels: (1) differences between types of VLM estimates: (i) VLM_{GPS} mainly assuming linear processes, (ii) VLM_{ATG} including all processes, linear and non-linear and (iii) VLM_{GIA} that obviously include only the GIA, which is linear over the time periods considered here; (2) differences between GPS products: SONEL and NGL; and (3) differences between altimetry products: AVISO and CSIRO. Not surprisingly, the largest discrepancies were found at the first level, i.e. when the different types of VLM were compared, not only when VLM_{GIA} estimates were compared to the two others, but also when VLM_{GPS} and VLM_{ATG} (both including GIA and non-GIA VLM) estimates were compared (see Fig. 3c). In addition, the GIA model is not intended to account for any process different than GIA, which in turn has a weak impact (mainly uplift) over the study domain.

Figure 4 shows a comparison of the VLM time series obtained from the difference between altimetry and TG data and those obtained from the GPS analysis centres. It can be seen that ATG time series, at those stations where discrepancies between weighted averaged VLM_{ATG} and VLM_{GPS} are important (Lautoka, Funafuti, Papeete, Rikitea, Noumea A, Norfolk Island and Nukulaofa), present non-linear oscillations that do not appear in the GPS time series. Another example is Port Vila B (Vanuatu), where SONEL and NGL did not provide robust VLM trend estimates, and where we found that the tide gauge uplift over the altimetry period (1.7 ± 0.2 mm/y) may have been mainly produced by the effect of earthquakes that can impact the land motion in the area (Ballu et al., 2011). At the stations where VLM linear trends from SONEL were not assessed as robust (Suva, Apia B and Pago Pago), both VLM_{GPS} time series from NGL were more similar to that for VLM_{ATG}, which is not surprising given that the GPS position time series provided by NGL include the offsets. It is especially evident at Apia B and Pago Pago, where VLM_{ATG} and VLM_{GPS} time series present the impact (co-seismic and post-seismic signal) of a large earthquake which occurred in 2009 (Okal et al., 2010) due to the bending of the plate entering the Tonga-Kermadec subduction zone.

We explored the impact of the uncertainty associated with the different VLM estimates to explain the RSL trends by comparing the RSL trends estimated from the TG records over the 1993-2015 period with those calculated from differenced (satellite altimetry minus VLM) trends. VLM_{GPS} (SONEL, NGL and their weighted mean) and VLM_{GIA} trends were used here (see Fig. S5). RSL trends obtained from satellite altimetry minus weighted averaged VLM_{GPS} were similar to the tide gauge RSL trends in most of the cases except at some locations where tide gauge RSL trends were either overestimated, as at Noumea A and Papeete (PAPE), or underestimated, as at Norkfolk Island and Nukulaofa. Similar results were found when VLM_{GPS} from SONEL and NGL were used separately, except for Papeete (PAPE), where the observed RSL trend was not significantly overestimated for NGL. RSL trends obtained from VLM_{GIA} were similar to the tide gauge trends at most of the cases, except for some stations, namely Norfolk Island, Pago Pago and Apia B, where observed RSL trends where highly underestimated which is not surprising given that the GIA model is not intended to account for the strong subsidence of tectonic origin observed in these stations.

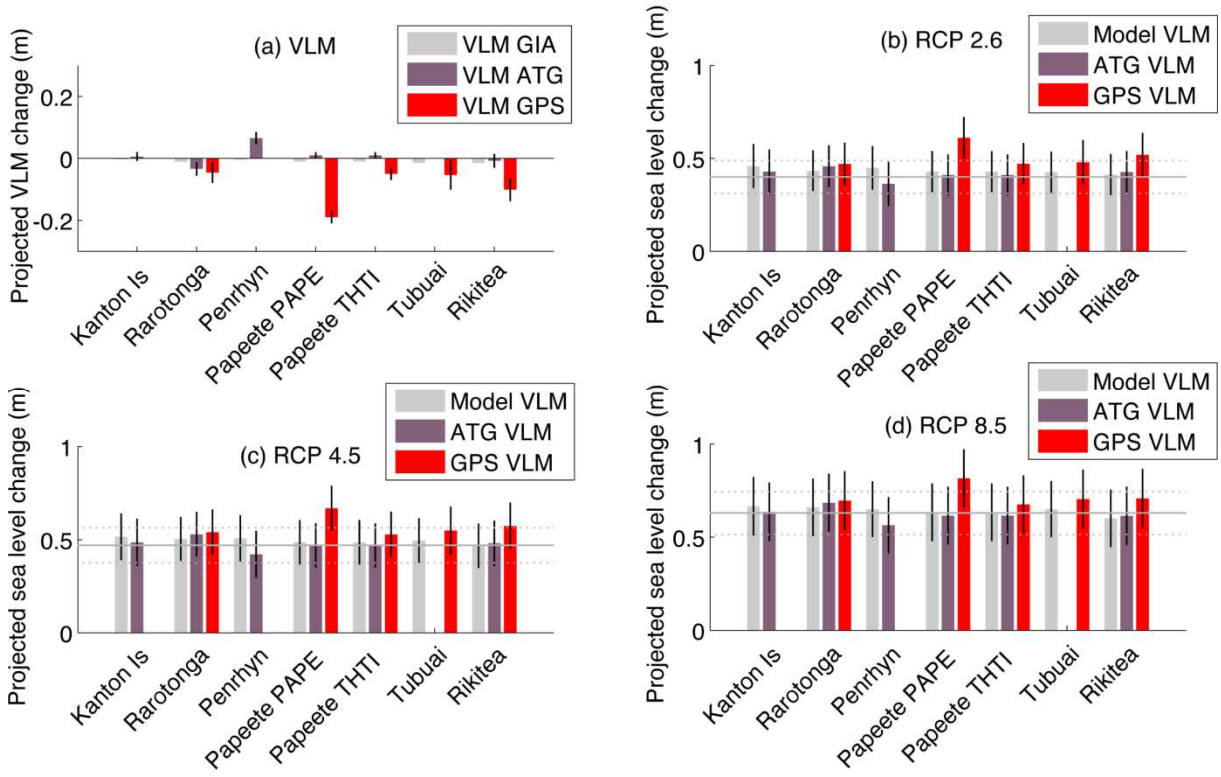

564
565
566 **Figure 5.** (a)Vertical land motion change (m) over the twenty-first century (2081-2100 mean
567 minus the 1986-2005 mean) obtained from the GIA model (light grey bars), weighted
568 averaged VLM_{ATG} (purple bars) and VLM_{GPS} (red bars) at the locations with no-evidence of
569 earthquakes. Error bars (vertical black lines) denote standard errors. Projected relative sea-
570 level changes over the twenty-first century under (b) the RCP 2.6, (c) RCP 4.5and (d) RCP
571 8.5 including VLM projected changes. Horizontal lines denote the global mean sea-level
572 changes over the twenty-first century and their standard errors.
573
574

575 We illustrated that VLM linear trend estimates from both GPS data and the GIA model may
576 underestimate the observed RSL changes at locations where non-linear VLM occur. However,
577 when it comes to obtaining future projections of RSL, VLM estimates including non-GIA
578 effects are needed. The question arises how projectable into the future are VLM estimates, in
579 particular in the presence of non-linear processes. One can assume that only linear processes
580 are reasonably projectable into the future, however it is very difficult to assess that estimated
581 VLM_{GPS} result from a combination of only linear processes. Given that earthquakes are not
582 predictable, it is not suitable to use any observed VLM estimates to obtain RSL projections at
583 locations where there is evidence of earthquakes of any magnitude. That does not, however,
584 prevent that where there is no observational evidence of earthquakes, other unpredictable non-
585 linear processes could arise. In spite of the necessary caution of the outcome, we projected the
586 linear estimates of our VLM to obtain RSL changes by the end of the 21st Century under three

587 different GHG emission scenarios at a subset of 7 selected locations where no evidence of
588 non-linear processes, especially earthquakes, was found in both GPS data centres. These sites
589 are located far from active tectonic boundaries. We implicitly assumed that observed VLM,
590 when they are linear, will continue along the 21st Century (see Fig. 5a). Results at this region
591 revealed no significant differences between projected RSL that accounted for all vertical
592 movements (including both GIA and non-GIA) and projected RSL that only account for GIA
593 motions, with the exception of Papeete, where projected sea-level changes accounting for
594 VLM_{GPS} (0.8 ± 0.2 m under RCP 8.5) were significantly higher than those obtained with
595 VLM_{GIA} (0.6 ± 0.2 m) and VLM_{ATG} (0.6 ± 0.2 m) under the three GHG scenarios (see Fig.
596 5b-c). The Tahiti case requires more research to elucidate the high discrepancies in the VLM
597 estimates between the two GPS stations located there, which could be revealing the strong
598 local differences of VLM that can be found even within the same island. RSL at the
599 remaining locations is expected to rise in a similar way than the global sea level rise along the
600 21st century with values of 0.4 ± 0.2 m, 0.5 ± 0.2 m and 0.6 ± 0.2 m for the RCP2.6, RCP4.5
601 and RCP8.5 scenarios, respectively.
602
603 **6. Conclusion**
604 Previous studies on the impact of vertical land motion (VLM) on sea-level changes over the
605 South Western Tropical Pacific Islands predominantly focused on specific islands or
606 archipelagos and/or lacked deep analysis of the uncertainties associated. Moreover, they have
607 not assessed whether reliable future relative sea level projections can be obtained on the basis
608 of the vertical land motion estimates.
609 We have investigated present and future relative sea level (RSL) changes at as many islands
610 as possible over the region and for this, we have quantitatively analyzed the uncertainties and
611 nature of the vertical land movements. We found that, on the long term (last 4-6 decades), the
612 relative sea level has increased more than globally over this region, confirming the results of
613 Becker et al., 2012. Moreover, we found the highest increases at the islands located over the
614 central part of the South Western Tropical Pacific, mainly due to the vertical land movements
615 produced by the high tectonic activity in this area, which limits our ability to obtain reliable
616 future RSL projections, but highlights the importance for the populations in earthquake prone
617 areas to be aware of the potential contribution of vertical land motion to future RSL changes.
618 We also found that the eastern islands, located in the tectonically inactive areas, experienced
619 vertical land movements of higher magnitude than those produced by the GIA. However,
620 although RSL projections obtained there are better constrained, they generally show a similar

rise than globally over the 21st century (0.6 ± 0.2 m under RCP8.5 scenario), with the exception of Papeete (Tahiti), where future relative sea level projections obtained by considering the subsidence registered at a GPS station (PAPE) show much larger rises (0.8 ± 0.2). Strong differences between these two types of vertical land motion estimates were also observed for most of the islands located over the region indicating that future work should show if these differences can be linked to the high spatial variability of vertical land movements at local scale or due to the data processing.

From a more policy perspective, two benefits are to be expected from better including vertical land motion (sources, rates, and uncertainty) in projections on future sea-level rise, i.e. move towards more reliable future RSL projections. First, this would help refining the projections. While projections of global mean sea-level rise are critical to raise the issue worldwide, refined information is needed locally to estimate context-specific vulnerability to sea-level rise and design robust adaptation strategies. This is especially true for the South Western Tropical Pacific that is at the frontline of climate change. Second, this would help improving confidence in projections. Including vertical land motion into projections of future sea level will not be a straightforward exercise, as suggested in this study, and more local scale projections will still be accompanied with uncertainty, for instance related to the occurrence of earthquakes that are important contributors to vertical land motion in some areas. However, better capturing the contribution of vertical land motion to future relative sea-level rise would help providing levels of confidence on future sea level rise projections, from moderate confidence in areas that are highly affected by vertical land motion mainly due to earthquakes, to higher confidence in areas where vertical land motion are dominated by more gradual and predictable drivers.

Acknowledgements

This study benefited from the support of the French National Research Agency (ANR) under the *Storisk* research project (ANR-15-CE03-0003). We thank the University of Hawaii Sea Level Center (http://uhslc.soest.hawaii.edu/), the Permanent Service of Mean Sea Level (http://www.psmsl.org/) and the Système d'Observation du Niveau des Eaux Littorales (http://www.sonel.org/) for providing us tide gauge data. We thank AVISO (http://www.aviso.altimetry.fr) and CSIRO (http://www.cmar.csiro.au/sealevel/sl_data_cmar.html) for the satellite radar altimetry data, the Système d'Observation du Niveau des Eaux Littorales (http://www.sonel.org/) and the Nevada Geodetic Laboratory (http://geodesy.unr.edu/) for the GPS data. Bathymetry was

obtained from the GEBCO Digital Atlas published by the British Oceanographic Data Centre, on behalf of IOC and IHO, 2003 (http://www.gebco.net). We sincerely thank Dr Álvaro Santamaría-Gómez for his help and support during the early phases of this work. The authors would also like to acknowledge comments received from the anonymous reviewers, which led to significant improvements of the paper.

Supplementary material

Table S1. RSL trend uncertainties defined as the SE of the fit adjusted for lag-1 autocorrelation for monthly and annually averaged time series at each tide gauge location. Only years containing more than 10 valid months were considered.

		SE adjusted (mm/year)	
Tide gauge	Total period	Monthly data	Annual data
Anewa Bay	1968-1977	13.7	7.1
Honiara	1974-2015	1.9	1.5
Noumea A	1967-2015	0.4	0.6
Ouinne	1981-2015	0.3	0.3
Nauru	1974-2014	1.0	1.0
Lifou	2011-2015	9.7	7.2
Norfolk Is	1994-2014	2.1	3.4
Port Vila VU A	1977-1982	16.1	-
Port Vila VU B	1993-2015	1.3	2.2
Lautoka	1992-2014	1.5	1.4
Suva	1972-2015	0.7	1.1
Funafuti	1977-2015	1.3	0.9
Nukualofa	1993-2014	1.1	1.6
Apia A	1954-1971	1.6	1.7
Apia B	1993-2015	2.2	1.6
Kanton Is	1949-2012	0.5	0.7
Pago Pago	1948-2014	0.5	0.5
Rarotonga	1977-2015	0.5	0.6
Penrhyn	1977-2015	0.8	1.0
Papeete	1969-2014	0.4	0.5
Matavai	1958-1967	2.0	0.8
Tubuai	2009-2013	15.1	9.1
Rangiroa	2009-2014	6.0	23.4
Nuku Hiva	1982-2015	1.3	0.8
Hiva Oa A	1977-1980	8.9	-
Hiva Oa B	2010-2015	9.4	3.3
Rikitea	1969-2015	0.3	0.3
MEAN		3.7	2.9

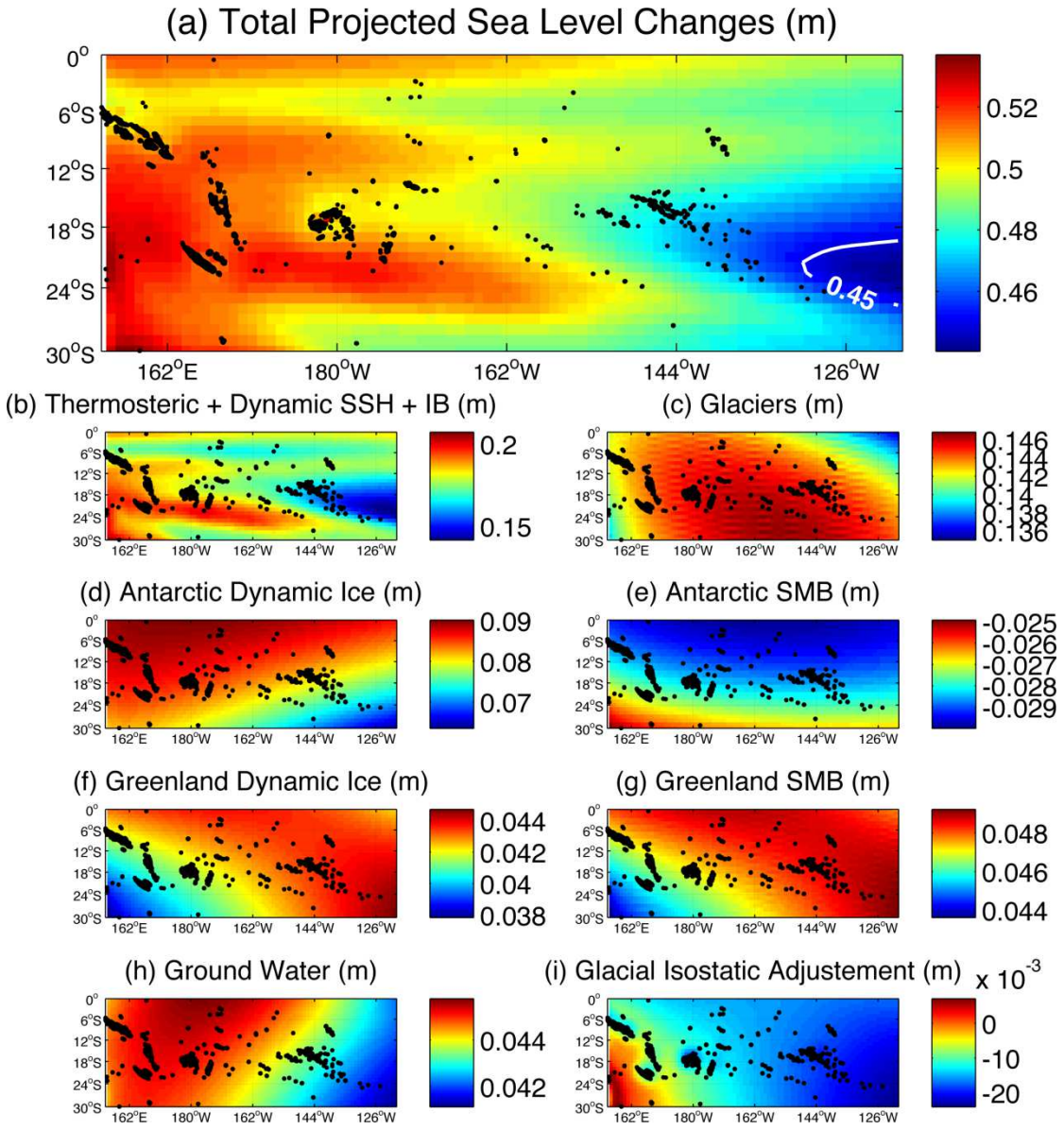

Figure S1. Regional sea-level changes of the different sea level contributions from RCP8.5 over the period from 1986–2005 to 2081–2100 (in meters). Total projected regional sea-level changes resulting from the sum of all the contributions (a). The CMIP5-RCP8.5 ensemble mean of the sum of the thermosteric, dynamic and atmospheric (b), glacier (c), ice sheet (d-g), groundwater (h) and GIA (i) contributions.

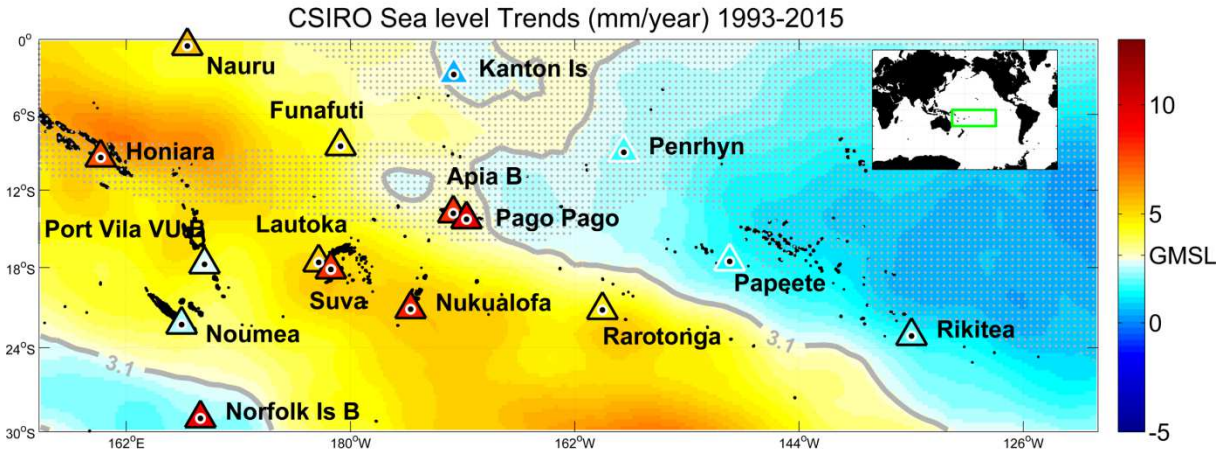

Figure S2. Sea level trends (mm/year) at tide gauges (coloured triangles) and CSIRO altimetry grid points (coloured areas) calculated over 1993-2015. Grey contours mark global mean sea level trend during 1993-2015. White-bordered triangles and dot-shaded areas denote no statistical significance at 2σ level.

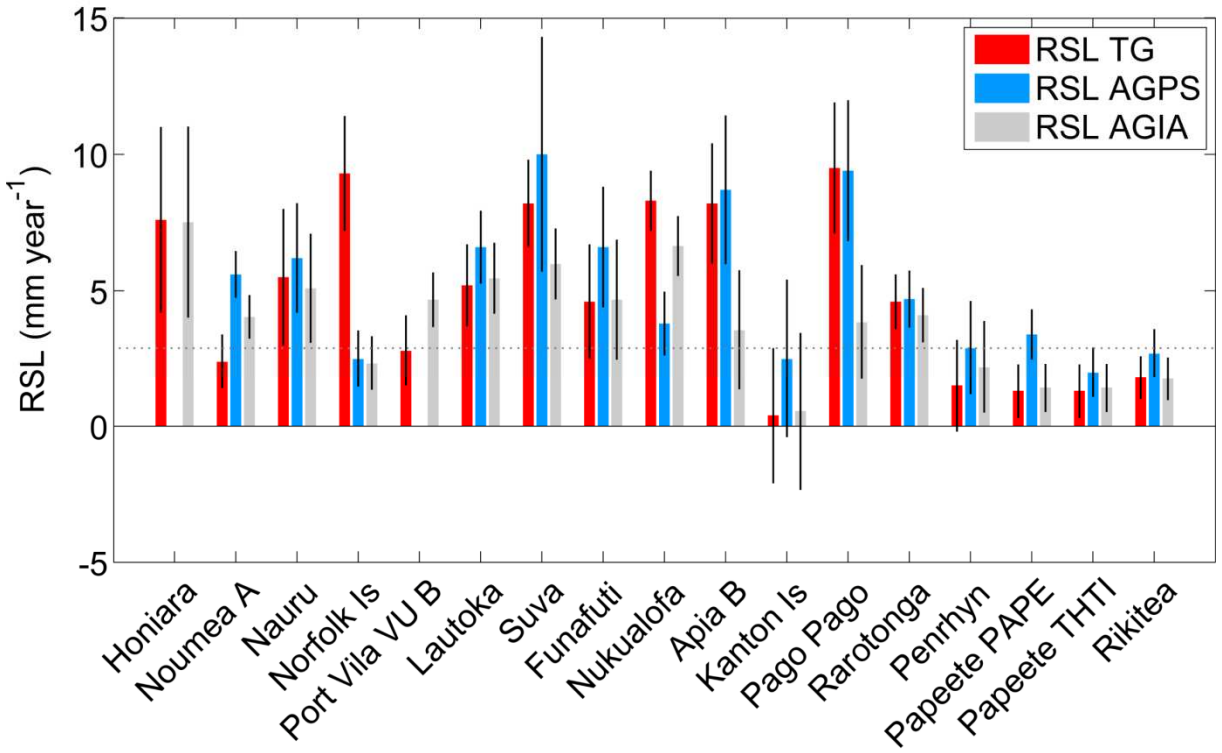

Figure S3. RSL TG: Trends of relative sea level from tide gauges records (red bars), satellite radar altimetry (AVISO) minus weighted averaged VLM_{GPS} trends (blue bars) and satellite radar altimetry (AVISO) minus modelled VLM_{GIA} (grey bars). Error bars denote one standard error of the trends.

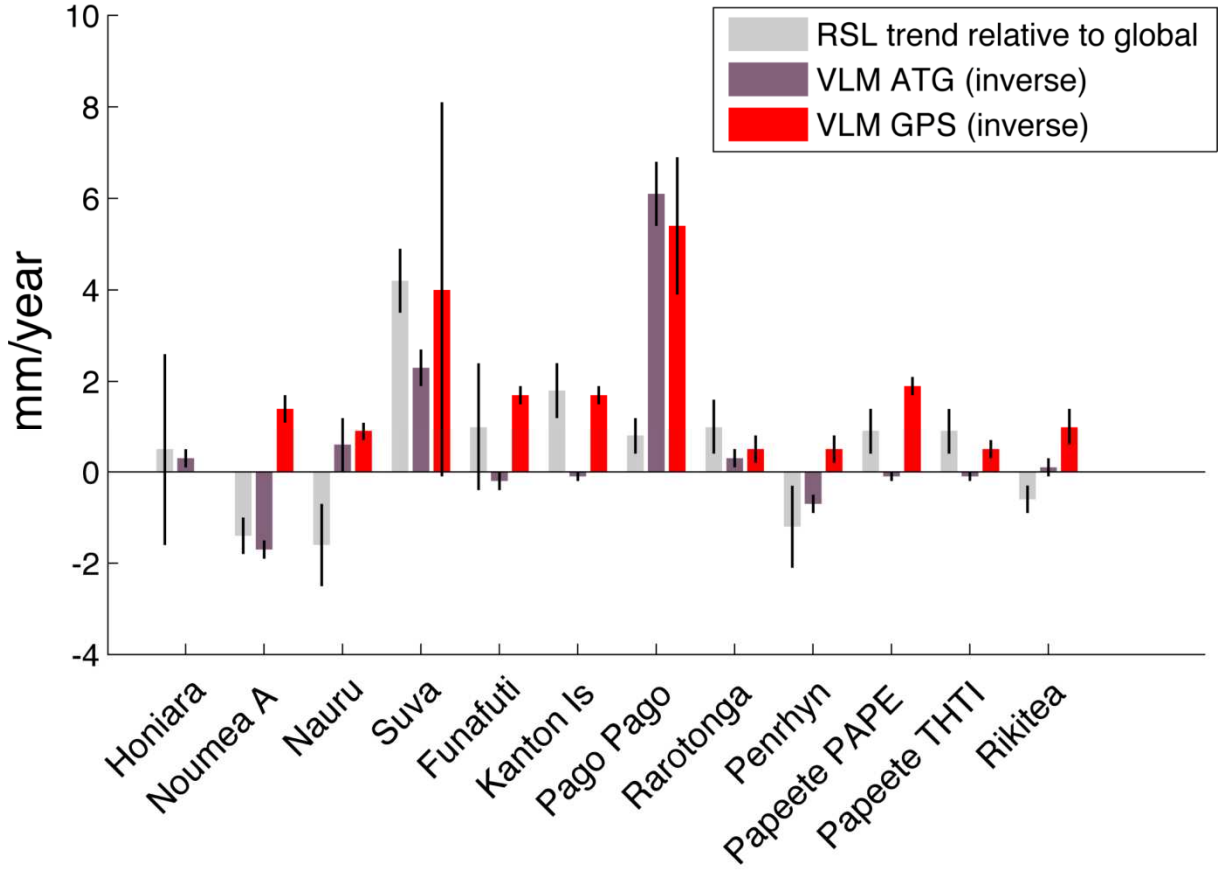

Figure S4. Difference between local RSL trends and global mean sea-level rise (mm/year) at the longest tide gauges (light grey bars). Inverse of the vertical land motion rate (mm/year) obtained from weighted averaged VLM_{ATG} (purple bars) and VLM_{GPS} (red bars). Error bars (vertical black lines) denote standard errors.

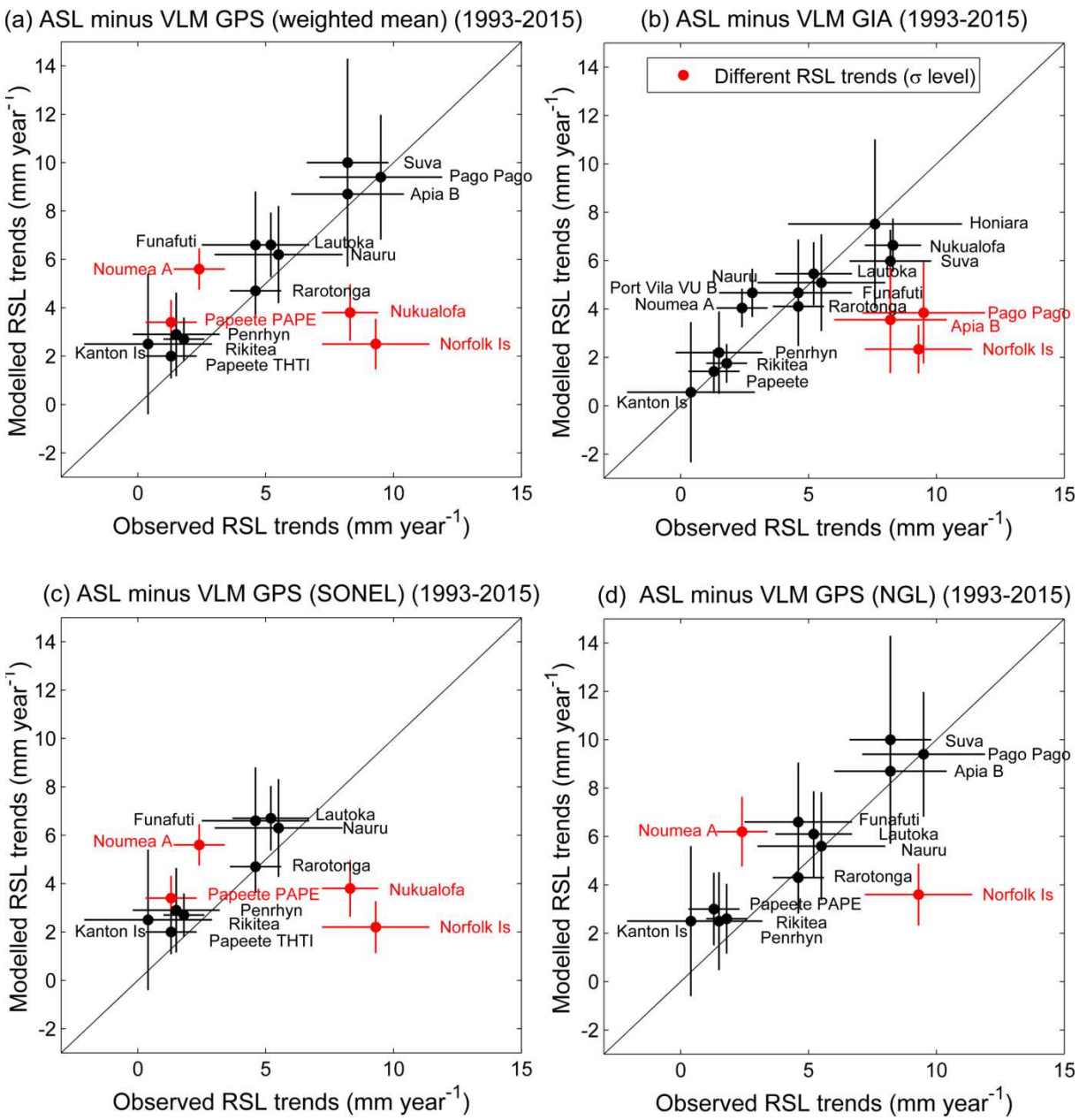

Figure S5. Scatterplot between observed and modelled RSL trends obtained from ASL trends (AVISO) minus vertical land motion trends from weighted mean VLM_{GPS} trends (a), VLM_{GIA} trends (b) and VLM_{GPS} trends from SONEL (c) and NGL (d). Error bars denote one σ standard error of the trends. Red dots and bars denote different trends at σ significance level (T-test).

References

Adam, C., Yoshida, M., Suetsugu, D., Fukao, Y., & Cadio, C. (2014). Geodynamic modeling of the South Pacific superswell. Physics of the Earth and Planetary Interiors, 229, 24-39.

Aung, T. H., Singh, A. M., & Prasad, U. W. (2009). Sea level threat in Tuvalu. American Journal of Applied Sciences, 6(6), 1169-1174.

Bamber, J. L., & Aspinall, W. P. (2013). An expert judgement assessment of future sea level rise from the ice sheets. Nature Climate Change, 3(4), 424-427.

Barnard P.L., Short A.D., Harley M.D., Splinter K., Vitousek S., Turner I., Allan J., Banno M., Bryan K., Doria A., Hansen J., Kato S., Kuriyama Y., Randall-Goodwin E., Ruggiero P., Walker P., Heathfield D. (2015). Coastal vulnerability across the Pacific dominated by El Niño/Southern Oscillation. Nature Geoscience, 8(10), 801-807.

Becker, M., Meyssignac, B., Letetrel, C., Llovel, W., Cazenave, A., & Delcroix, T. (2012). Sea level variations at tropical Pacific islands since 1950. Global and Planetary Change, 80, 85-98.

Ballu, V., Bouin, M. N., Siméoni, P., Crawford, W. C., Calmant, S., Boré, J. M., Kanas, T., & Pelletier, B. (2011). Comparing the role of absolute sea-level rise and vertical tectonic motions in coastal flooding, Torres Islands (Vanuatu). Proceedings of the National Academy of Sciences, 108(32), 13019-13022.

Blewitt, G., C. Kreemer, W.C. Hammond, J. Gazeaux, 2016, MIDAS robust trend estimator for accurate GPS station velocities without step detection, accepted for publication in the Journal of Geophysical Research, doi: 10.1002/2015JB012552.

Bromirski, P. D., Miller, A. J., Flick, R. E., & Auad, G. (2011). Dynamical suppression of sea level rise along the Pacific coast of North America: Indications for imminent acceleration. Journal of Geophysical Research: Oceans, 116(C7).

Carson, M., A. Koehl, D. Stammer, A.B.A. Slangen, C.A. Katsman, R.S.W. van de Wal, J. A. Church, N. White (2016) Coastal Sea Level Changes, Observed and Projected during the 20th and 21st Century, Climatic Change, 134 (1), 269-281.

Cazenave, A., K. Dominh, F. Ponchaut, L. Soudarin, J.-F. Cretaux, & C. Le Provost (1999), Sea level changes from Topex–Poseidon altimetry and tide gauges, and vertical crustal motions from DORIS, Geophys. Res. Lett., 26, 2077–2080.

748 Cazenave, A., & Cozannet, G. L. (2014). Sea level rise and its coastal impacts. Earth's
749 Future, 2(2), 15-34.

750 Church, J. A., White, N. J., & Hunter, J. R. (2006). Sea-level rise at tropical Pacific and
751 Indian Ocean islands. Global and Planetary Change, 53(3), 155-168.

752 Church, J. A., & White, N. J. (2011). Sea-level rise from the late 19th to the early 21st
753 century. Surveys in Geophysics, 32(4-5), 585-602.

754 Church, J. A., P. Clark, A. Cazenave, J. Gregory, S. Jevrejeva, A. Levermann, M. Merrifield,
755 G. Milne, R.S.Nerem, P. Nunn, A. Payne, W. Pfeffer, D. Stammer, & A.
756 Unnikrishnan (2013a). Sea level change, in Climate Change 2013: The Physical
757 Science Basis, edited by T. F. Stocker, D. Qin, G.-K. Plattner, M. Tignor, S. Allen,
758 J. Boschung, A. Nauels, Y. Xia, V. Bex, & P. Midgley, Cambridge University Press,
759 Cambridge, UK and New York, NY. USA

760 Church, J.A., P.U. Clark, A. Cazenave, J.M. Gregory, S. Jevrejeva, A. Levermann, M.A.
761 Merrifield, G.A. Milne, R.S. Nerem, P.D. Nunn, A.J. Payne, W.T. Pfeffer, D.
762 Stammer & A.S. Unnikrishnan (2013b). Sea Level Change Supplementary Material.
763 In: Climate Change 2013: The Physical Science Basis. Contribution of Working
764 Group I to the Fifth Assessment Report of the Intergovernmental Panel on Climate
765 Change [Stocker, T.F., D. Qin, G.-K. Plattner, M. Tignor, S.K. Allen, J. Boschung,
766 A. Nauels, Y. Xia, V. Bex & P.M. Midgley (eds.)].

767 Connell, J. (2015). Vulnerable Islands: climate change, tectonic change, and changing
768 livelihoods in the Western Pacific. the contemporary pacific, 27(1), 1-36.

769 DeConto, R. M., & Pollard, D. (2016). Contribution of Antarctica to past and future sea-level
770 rise. Nature, 531(7596), 591-597.

771 Duvat, V.K.E., 2018. A global assessment of atoll island planform changes over the past
772 decades. WIREs Climate Change ww.557. doi: 10.1002/wcc.557

773 Duvat, V. K.E., Magnan, A. K., Wise, R. M., Hay, J. E., Fazey, I., Hinkel, J., Stojanovic, T.,
774 Yamano, H. & Ballu, V. (2017). Trajectories of exposure and vulnerability of small
775 islands to climate change. WIREs Clim Change, e478. doi:10.1002/wcc.478

776 Fadil, A., Sichoix, L., Barriot, J. P., Ortéga, P., & Willis, P. (2011). Evidence for a slow
777 subsidence of the Tahiti Island from GPS, DORIS, and combined satellite altimetry
778 and tide gauge sea level records. Comptes Rendus Geoscience, 343(5), 331-341.

779 Featherstone, W. E., Penna, N. T., Filmer, M. S., & Williams, S. D. P. (2015). Nonlinear
780 subsidence at Fremantle, a long□recording tide gauge in the Southern
781 Hemisphere. Journal of Geophysical Research: Oceans, 120(10), 7004-7014.

782 Gazeaux, J., Williams, S., King, M., Bos, M., Dach, R., Deo, M., Moore, A.W., Ostini, L.,
783 Petrie, E., Roggero, M., Teferle, F.N., Olivares, G., Webb, F.H., 2013: Detecting
784 offsets in GPS time series: First results from the detection of offsets in GPS
785 experiment, Journal of Geophysical Research B: Solid Earth.

786 Hamlington, B. D., Leben, R. R., Nerem, R. S., Han, W., & Kim, K. Y. (2011).
787 Reconstructing sea level using cyclostationary empirical orthogonal
788 functions. Journal of Geophysical Research: Oceans, 116(C12).

789 Hamlington, B. D., Strassburg, M. W., Leben, R. R., Han, W., Nerem, R. S., & Kim, K. Y.
790 (2014). Uncovering an anthropogenic sea-level rise signal in the Pacific
791 Ocean. Nature Climate Change, 4(9), 782-785.

792 Han, G., Ma, Z., Chen, N., Yang, J., & Chen, N. (2015). Coastal sea level projections with
793 improved accounting for vertical land motion. Scientific reports, 5.

794 Han, W., Meehl, G. A., Stammer, D., Hu, A., Hamlington, B., Kenigson, J., Kenigson, H.,
795 Palanisamy, H., & Thompson, P. (2017). Spatial patterns of sea level variability
796 associated with natural internal climate modes. Surveys in Geophysics, 38(1), 217-
797 250.

798 Hay, C. C., Morrow, E., Kopp, R. E., & Mitrovica, J. X. (2015). Probabilistic reanalysis of
799 twentieth-century sea-level rise. Nature, 517(7535), 481-484.

800 Holgate, S., Matthews, J., A., Woodworth, P. L., Rickards, L. J., Tamisiea, M. E.,
801 Bradshaw, E., Foden, P. R., Gordon, K. M., Jevrejeva, S. & Pugh, J. (2013). New
802 data systems and products at the permanent service for mean sea level, J. Coastal
803 Res., 29(3), 493–504.

804 Jevrejeva, S., Jackson, L. P., Riva, R. E., Grinsted, A., & Moore, J. C. (2016). Coastal sea
805 level rise with warming above 2° C. Proceedings of the National Academy of
806 Sciences, 201605312.

807 Johnson, K.M. and Tebo, D. (2018). Capturing 50 years of postseismic mantle flow at Nankai
808 Subduction zone, 123, 10091-10106, Journal of Geophysical Research B: Solid
809 Earth, 10.1029/2018JB016345.

Keener, V. W., Marra, J. J., Finucane, M. L., Spooner, D., Smith, M. H., & Assessment, P. I. R. C. (2012). Climate change and Pacific islands: indicators and impacts: report for the 2012 Pacific Islands Regional Climate Assessment (PIRCA). Island Press, 170 pp.

Kopp, R. W., R. M. Horton, C. M. Little, J. X. Mitrovica, M. Oppenheimer, D. J. Rasmussen, B. H. Strauss, & C. Tebaldi (2014). Probabilistic 21st and 22nd century sea-level projections at a global network of tide gauge sites, Earth's Future, 2, 383–406,

Kopp R., DeConto, R. M., Bader, D., Horton, R. M., Hay, C. C., Kulp, S., Oppenheimer, M., Pollard, D., & Strauss, B. H. (2017). Implications of ice-shelf hydrofracturing and ice cliff collapse mechanisms for sea-level projections. https://arxiv.org/abs/1704.05597.

Le Cozannet, G., Garcin, M., Yates, M., Idier, D., & Meyssignac, B. (2014). Approaches to evaluate the recent impacts of sea-level rise on shoreline changes. Earth-Science Reviews, 138, 47-60.

Level, S. P. S. (2009). Climate Monitoring Project. 2006c. Pacific Country Report. Sea Level & Climate: Their Present State: Vanuatu.

Masters, D., Nerem, R. S., Choe, C., Leuliette, E., Beckley, B., White, N., & Ablain, M. (2012). Comparison of global mean sea level time series from TOPEX/Poseidon, Jason-1, and Jason-2. Marine Geodesy, 35(sup1), 20-41.

McLean, R., & Kench, P. (2015). Destruction or persistence of coral atoll islands in the face of 20th and 21st century sea□level rise?. Wiley Interdisciplinary Reviews: Climate Change, 6(5), 445-463.

McGregor, S., Gupta, A. S., & England, M. H. (2012). Constraining wind stress products with sea surface height observations and implications for Pacific Ocean sea level trend attribution. Journal of Climate, 25(23), 8164-8176.

McGregor, S., Timmermann, A., Stuecker, M. F., England, M. H., Merrifield, M., Jin, F. F., & Chikamoto, Y. (2014). Recent Walker circulation strengthening and Pacific cooling amplified by Atlantic warming. Nature Climate Change, 4(10), 888-892.

McNutt, M. K., & Fischer, K. M. (1987). The south Pacific superswell (pp. 25-34). American Geophysical Union.

841 Merrifield, M. A. (2011). A shift in western tropical Pacific sea level trends during the
842 1990s. Journal of Climate, 24(15), 4126-4138.

843 Merrifield, M. A., Thompson, P. R., & Lander, M. (2012). Multidecadal sea level anomalies
844 and trends in the western tropical Pacific. Geophysical Research Letters, 39(13).

845 Meyssignac, B., Becker, M., Llovel, W., & Cazenave, A. (2012). An assessment of two-
846 dimensional past sea level reconstructions over 1950–2009 based on tide-gauge data
847 and different input sea level grids. Surveys in Geophysics, 33(5), 945-972.

848 Moon, J. H., Song, Y. T., Bromirski, P. D., & Miller, A. J. (2013). Multidecadal regional sea
849 level shifts in the Pacific over 1958–2008. Journal of Geophysical Research:
850 Oceans, 118(12), 7024-7035.

851 Moss RH, Edmonds JA, Hibbard KA, Manning MR, Rose SK, van Vuuren DP, Carter TR,
852 Emori S, Kainuma M, Kram T, Meehl GA, Mitchell JFB, Nakicenovic N, Riahi K,
853 Smith SJ, Stouffer RJ, Thomson AM, Weynant JP, Wilbanks TJ (2010) The next
854 generation of scenarios for climate change research and assessment. Nature
855 463:747–756.

856 Nerem, R. S., Chambers, D. P., Choe, C., & Mitchum, G. T. (2010). Estimating mean sea
857 level change from the TOPEX and Jason altimeter missions. Marine
858 Geodesy, 33(S1), 435-446.

859 Nerem, R. S., & Mitchum, G. T. (2002). Estimates of vertical crustal motion derived from
860 differences of TOPEX/POSEIDON and tide gauge sea level
861 measurements. Geophysical Research Letters, 29(19).

862 Nicholls, R. J. (2011). Planning for the impacts of sea level rise. Oceanography, 24(2), 144-
863 157.

864 Nicholls, R. J., & Cazenave, A. (2010). Sea-level rise and its impact on coastal
865 zones. science, 328(5985), 1517-1520.

866 Nicholls, R. J., Hanson, S. E., Lowe, J. A., Warrick, R. A., Lu, X., & Long, A. J. (2014).
867 Sea□level scenarios for evaluating coastal impacts. Wiley Interdisciplinary
868 Reviews: Climate Change, 5(1), 129-150.

869 Nunn, P. D. (2009). Vanished islands and hidden continents of the Pacific. University of
870 Hawaii Press.

871 Nurse, L.A., McLean, R.F., Agard, J., Briguglio, L.P., Duvat-Magnan, V., Pelesikoti, N.,
872 Tompkins, E., Webb, A. (2014) Small islands. In: Barros, V.R., Field, C.B., Dokken,
873 D.J., Mastrandrea, M.D., Mach, K.J., Bilir, T.E., Chatterjee, M., Ebi, K.L., Estrada,
874 Y.O., Genova, R.C., Girma, B., Kissel, E.S., Levy, A.N., MacCracken, S.,
875 Mastrandrea, P.R., White, L.L. (eds) Climate Change 2014: Impacts, Adaptation,
876 and Vulnerability. Part B: Regional Aspects. Contribution of Working Group II to
877 the Fifth Assessment Report of the Intergovernmental Panel of Climate Change,
878 Cambridge University Press, Cambridge, pp 1613–1654.

879 Okal, E. A., Fritz, H. M., Synolakis, C. E., Borrero, J. C., Weiss, R., Lynett, P. J., ... & Chan,
880 I. C. (2010). Field survey of the Samoa tsunami of 29 September
881 2009. Seismological Research Letters, 81(4), 577-591.

882 Palanisamy, H., Cazenave, A., Delcroix, T., & Meyssignac, B. (2015). Spatial trend patterns
883 in the Pacific Ocean sea level during the altimetry era: the contribution of
884 thermocline depth change and internal climate variability. Ocean Dynamics, 65(3),
885 341-356.

886 Pelletier, B., Calmant, S. & Pillet, R. (1998) Current tectonics of the Tonga-New Hebrides
887 region. Earth Planet. Sci. Lett., 164, 263–276.

888 Peltier, W.R., Argus, D.F. & Drummond, R. (2015) Space geodesy constrains ice-age
889 terminal deglaciation: The global ICE-6G_C (VM5a) model. J. Geophys. Res. Solid
890 Earth, 120,450-487,

891 Perrette, M., Landerer, F., Riva, R., Frieler, K. & Meinshausen, M. (2013). A scaling
892 approach to project regional sea level rise and its uncertainties. Earth Syst Dyn
893 4:11–29.

894 Pfeffer, J., & Allemand, P. (2016). The key role of vertical land motions in coastal sea level
895 variations: A global synthesis of multisatellite altimetry, tide gauge data and GPS
896 measurements. Earth and Planetary Science Letters, 439, 39-47.

897 Pfeffer, J., Spada, G., Mémin, A., Boy, J. P., & Allemand, P. (2017). Decoding the origins of
898 vertical land motions observed today at coasts. Geophysical Journal
899 International, 210(1), 148-165.

900 Ray, R. D., & Douglas, B. C. (2011). Experiments in reconstructing twentieth-century sea
901 levels. Progress in Oceanography, 91(4), 496-515.

902 Rebischung, P., Altamimi, Z., Ray, J., & Garayt, B. (2016). The IGS contribution to
903 ITRF2014. Journal of Geodesy, 90(7), 611-630.

904 Ritz, C., Edwards, T. L., Durand, G., Payne, A. J., Peyaud, V., & Hindmarsh, R. C. (2015).
905 Potential sea-level rise from Antarctic ice-sheet instability constrained by
906 observations. Nature, 528(7580), 115.

907 Santamaría-Gómez, A., Gravelle, M., Dangendorf, S., Marcos, M., Spada, G., &
908 Wöppelmann, G. (2017). Uncertainty of the 20th century sea-level rise due to
909 vertical land motion errors. Earth and Planetary Science Letters, 473, 24-32.

910 Santer, B. D., Wigley, T. M. L., Boyle, J. S., Gaffen, D. J., Hnilo, J. J., Nychka, D., Parker, D.
911 E., & Taylor, K. E.: Statistical significance of trends and trend differences in layer-
912 average atmospheric temperature time series, J. Geophys. Res., 105, 7337- 7356.

913 Saunders, M. I., Albert, S., Roelfsema, C. M., Leon, J. X., Woodroffe, C. D., Phinn, S. R., &
914 Mumby, P. J. (2016). Tectonic subsidence provides insight into possible coral reef
915 futures under rapid sea-level rise. Coral Reefs, 35(1), 155-167.

916 Slangen, A. B. A., Carson, M., Katsman, C. A., Van de Wal, R. S. W., Köhl, A., Vermeersen,
917 L. L. A., & Stammer, D. (2014). Projecting twenty-first century regional sea-level
918 changes. Climatic Change, 124(1-2), 317-332.

919 Sun, C., Kucharski, F., Li, J., Jin, F. F., Kang, I. S., & Ding, R. (2017). Western tropical
920 Pacific multidecadal variability forced by the Atlantic multidecadal
921 oscillation. Nature communications, 8, 15998.

922 Tamisiea, M. E., & Mitrovica, J. X. (2011). The moving boundaries of sea level change:
923 Understanding the origins of geographic variability. Oceanography.

924 Taylor, F. W., R. W. Briggs, C. Frohlich, A. Brown, M. Hornbach, A. K. Papabatu, A. J.
925 Meltzner, & D. Billy (2008). Rupture across arc segment and plate boundaries in the
926 1 April 2007 Solomons earthquake, Nat. Geosci., 1(4), 253–257.

927 Taylor, F. W., Isacks, B. L., Jouannic, C., Bloom, A. L., & Dubois, J. (1980). Coseismic and
928 Quaternary vertical tectonic movements, Santo and Malekula Islands, New Hebrides
929 island arc. Journal of Geophysical Research: Solid Earth, 85(B10), 5367-5381.

930 Taylor, K. E., Stouffer, R. J., & Meehl, G. A. (2012). An overview of CMIP5 and the
931 experiment design. Bulletin of the American Meteorological Society, 93(4), 485-
932 498.

933 Thompson, P. R., Merrifield, M. A., Wells, J. R., & Chang, C. M. (2014). Wind-driven
934 coastal sea level variability in the northeast pacific. Journal of Climate, 27(12),
935 4733-4751.

936 Timmermann, A., McGregor, S., & Jin, F. F. (2010). Wind effects on past and future regional
937 sea level trends in the southern Indo-Pacific. Journal of Climate, 23(16), 4429-4437.

938 Volkov, D.L., Larnicol, G., & Dorandeu, J. (2007). Improving the quality of satellite altimetry
939 data over continental shelves. Journal of Geophysical Research. 112, C06020.

940 Weatherall, P., Marks, K.M., Jakobsson, M., Schmitt, T., Tani, S., Arndt, J.E., Rovere, M., et
941 al. (2015) A new digital bathymetric model of the world's oceans. Earth Sp. Sci., 1–
942 15. doi:10.1002/2015EA000107.

943 Wöppelmann, G., & Marcos, M. (2016). Vertical land motion as a key to understanding sea
944 level change and variability. Reviews of Geophysics, 54(1), 64-92.

945 Widlansky, M. J., Timmermann, A., & Cai, W. (2015). Future extreme sea level seesaws in
946 the tropical Pacific. Science advances, 1(8), e1500560.

947 Zhang, X., & Church, J. A. (2012). Sea level trends, interannual and decadal variability in the
948 Pacific Ocean. Geophysical Research Letters, 39(21).
949
950
951
952
953